الجمهورية الجزائرية الديمقراطية الشعبية
Democratic and Popular Republic of Algeria
وزارة التعليم العالي والبحث العلمي
Ministry of Higher Education and Scientific Research
جامعة الشهيد الشيخ العربي التبسي - تبسة
Shahid Sheikh Larbi Tébessi University– Tébessa –
Faculty of Science and Technology
Civil Engineering Department

Master Academic Dissertation

In Structures Engineering

Academic year: 2024/2025

By: BAKHOUCHE SARA

Theme

LINEAR AND NON-LINEAR STUDY OF THE LATERAL DISTORSIONAL BUCKLING OF CASSTELLATED STEEL BEAM

Presented on June, the 10th 2025

Examination board

Prof. E.H. Harkati	President
Dr. A. Boudjellal.	Examiner
Dr. LABED Abderrahim	Supervisor

Promotion: 2024/2025


بسم الله الرحمن الرحيم
١٤٣٨

Acknowledgement

وَمَا تَوْفِيقِي إِلَّا بِاللَّه – هود 88

First and foremost, I would like to thank Allah for giving me the strength, patience and determination to finish this academic journey, despite the many challenges I encountered along the way.

I would also like to express my heartfelt gratitude to my supervisor, Dr Abderrahim Labed, for his continuous support, insightful guidance, and unwavering trust throughout this project. His precise comments, thoughtful suggestions and willingness to help were invaluable in ensuring the progress and quality of this research. I am truly thankful for his patience in answering my frequent questions, for encouraging me during moments of doubt, and for his commitment to helping me structure and develop my ideas. I have learnt a great deal from him, both academically and personally, and I will always be inspired by his mentorship in my future endeavours.

I would also like to thank the members of the defence committee for reading and evaluating this work and for providing valuable feedback.

My thanks also go to the Department of Civil Engineering its administration, professors and staff for their academic support and efficient organisation, and for providing a stimulating learning environment throughout my years of study. Finally, I would like to thank all the teachers and fellow students I met during my studies for the enriching discussions, collaborative spirit and unforgettable experiences.

My deepest thanks go to my dear family, especially my parents, for their unwavering love, sacrifices, and endless prayers. Thank you to my mother for her tenderness and encouragement, and to my father for his unshakable support and constant provision-both material and emotional.

I also extend sincere thanks to my brothers and sisters, who were always there to lift my spirits, encourage me, and remind me of the purpose behind my efforts. Their support and presence have meant more than words can express.

To my friends and colleagues, thank you for sharing the journey-your support, humour, and companionship helped me overcome the difficult moments. I am grateful for the laughter, the shared efforts, and the motivation that you provided along the way.

I also extend sincere thanks to my brothers and sisters, who were always there to lift my spirits, encourage me, and remind me of the purpose behind my efforts. Their support and presence have meant more than words can express.

To my friends and colleagues, thank you for sharing the journey-your support, humour, and companionship helped me overcome the difficult moments. I am grateful for the laughter, the shared efforts, and the motivation that you provided along the way.

Finally, a simple but sincere word of thanks to myself, because despite the pressure, fatigue, and sleepless nights, I was able, by the grace of God, to persevere and achieve this achievement.

Dedication

After a journey that lasted for years, during which I carried a lot of difficulties, hardship and fatigue, here I am today, standing on the threshold of my graduation, reaping the fruits of my toil and raising my hat with pride. Praise be to you before you are satisfied, praise be to you if you are satisfied, and praise be to you after satisfaction, because you helped me to complete this work and fulfill my dream.

I dedicate this success to the one who decorated my name with the most beautiful titles, who supported me without limits and gave me free of charge, to the one who taught me that the world is a struggle and its weapon is science and knowledge, to the one who instilled in my soul morals, my first supporter in my journey, my strength and my support after God to my pride and pride, my father Abdel kader

To the one who made paradise under her feet and embraced me with her heart before her hands and facilitated my hardships with her prayers

The tender heart and the candle that was for me in the dark nights, the secret of my strength and success, and the lamp of my path that illuminated my life, my mother Hassina

My sister Zainab, my brother Osama and Elias, the apple of my eye, and my sister Zeyneb, my brother Ossama and Ilyes.

You have always been the light that illuminates my path, and the pillar that I lean on when the days tilt. Your support, words, and attitudes were the balm in my moments of weakness, and with you, the meaning of family is complete and the heart blooms. You have a share in this success, and I have indescribable love and endless gratitude in my heart.

I dedicate to you this achievement and the fruit of my success that I have always wished for, and today I have completed the first fruits of it, hoping that God Almighty will benefit me with what you taught me, teach me what I do not know, and make it an argument for me and not against me.

Bakhouche Sara

List of Symbol	Designation
A	Cross sectional area
E	Elastic modulus of steel
fy	Material yield stress.
G	the shear modulus of elasticity of steel,
ν	Poisson's ratio
W_{PL}	plastic module of the unperforated cross section
J	torsional constant
Cw	warping constant
Iy	the out of plane moment of inertia
l	length of unbraced portion of beam
h	distance between flange centroids
w	web thickness
h_w	Clear web depth between flanges
ϕ	angle (of inclined section to the vertical through the hole).
$V_{0,Rd}$	Resistance to the pure shear in the middle of the perforated section.
V_{sd}	Shear force.
M_{sd}	Applied global moment at the mid-length of the opening.
$M_{o,rd}$	moment resistance capacity
V_{h_i}	Longitudinal shear force at the welding joint of the web post.
$M_{N,el,Rd}$	Elastic resistant moment
Kt	Elastic or theoretical equivalent stress concentration factor
h	Total height
t_w	Web thickness.
t_f	Flange thickness.

b	Flange width
I_y	Moment of inertia
I_Z	Moment of inertia
I_t	Inertia of torsion
I_w	Factor of warping
r_o	Fillet radius of the rolled section
do	Circular opening diameter.
h_0	Height of the opening
l_o	Opening length
L	Length of beam
p	Loading
μ_{cr}	Buckling mode coefficient
p_{cr}	Critical load
M_{cr}	elastic critical moment capturing the effects of distortional buckling
P_0	dead load (initial load applied before the RIKS step)
P_{ref}	reference load (the load pattern applied in the step)
P_{tot}	Total load vector
λ	load proportionality factor
K_0	Stiffness matrix of the structure in the initial state.
λ_i	Eigenvalue

LIST OF TABLES

Title	Page
Table 1.1Variation of geometric dimensions of cellular beams according to application and objective	**10**
Table 4.1 Profile geometrical properties	**57**
Table 4.2 Perforated profile geometrical properties	**57**
Table 4.3 Geometrical details of web openings	**58**
Table 4.4 Validation of numerical models Abaqus vs. LTBeam model	**59**
Table 4.5 Effect of a single opening on LTB resistance of WEB	**60**
Table 4.6 Effect of multi -openings on LTB resistance of WEB	**61**

LIST OF FIGURES

Titles of respective Figures	page
Figure 1.1: Four Stages of formation of a castellated beam	**2**
Figure 1.2: Structural components of a castellated beam	**3**
Figure 1.3 : Various web opening shapes in floor beams.	**4**
Figure 1.4: Application fields of cellular beams: (a) service integration with ceiling attached to structure; (b) curved cellular beam roof structure, adapted from	**6**
Figure 1.5: Example of roof opening's beam applications	**7**
Figure 1.6 : Example of castellated beams	**7**
Figure 1.7: Example of cellular beams	**8**
Figure 1. 8: Beam with rectangular shape opening	**8**
Figure 1. 9: cellular beam with circular reinforcements	**8**
Figure 1. 10: rectangular shape with large reinforcement	**9**
Figure 1. 11: Ellipse openings	**9**
Figure 1. 12: Angelina beams	**10**
Figure 1. 13: Geometric dimensions of the cellular beam in front view	**11**
Figure 1. 14: geometry details of openings.	**11**
Figure 1 .15: Profile geometry of perforated cross section	**11**
Figure 1. 16:fabrication process of perforated steel beams.	**12**
Figure 1. 17: Fabrication process	**13**
Figure. 2.1: Cross-section during lateral torsional buckling at the initial configuration, at onset of buckling, and in the final position.	**15**
Figure 2.2: Buckling Modes in I Beams with a focus on distortion.	**16**
Figure 3.1: Effort distribution at the centre of the opening	**27**
Figure 3.2: Vierendeel bending and formation of four plastic hinges	**29**
Figure 3.3: Terminology characteristics of tested beam and views of the UG1 and VB-1 specimens	**31**
Figure 3.4: Stiffener anchorage length for horizontal stiffeners.	**31**
Figure 3.5: Bending failure of the beams with web-opening section	**33**
Figure 3.6: Moment distribution of local bending in the flanges	**34**
Figure 3.7: Local forces distribution at the corners of the opening	**34**
Figure 3.8: Plastic frame-type mechanism at the opening	**35**
Figure 3.9: Shear stress distribution (a) a solid web section (b) T-members	**36**
Figure 3.10: Principal compressive and tensile stresses in a panel and a beam with web openings under shear	**36**
Figure 3.11: Membrane action stresses in a plate under pure compression	**37**
Figure 3.12: Tensile diagonal field in a perforated panel	**37**
Figure 3.13: Buckling of the intermediate web post of a castellated beam	**38**
Figure 3.14: Beam tipping	**38**
Figure 3.15: Stress distribution in different parts of a component under various loading conditions: tension, bending, and torsion	**39**
Figure 4.1 Introducing boundary conditions and load	**48**

Figure 4.2 Introducing load position in the cross section	**48**
Figure 4.3 Calculation sheet from LTBEAM	**49**
Figure 4.4 Typical model with material and geometric properties	**52**
Figure 4.5 Setting-up the analysis	**53**
Figure 4.6 Defining the boundary conditions Boundary conditions	**53**
Figure 4.7 Defining the loads	**53**
Figure 4.8 Discretization	**54**
Figure 4.9 Visualisation and post- processing of the results	**55**
Figure 4.10 Linear buckling analysis deformed shape mode 1	**55**
Figure 4.11 Visualisation and post- processing of the results Mode 2	**56**
Figure 4.12 Discretization and Visualisation and post- processing of the results	**60**
Figure 4.13 Linear buckling analysis deformed shape modes 1and 2	**60**
Figure 4.14 Linear buckling analysis deformed shape mode 1 for square and rectangular openings	**61**
Figure 4.15 Discretization, Visualisation and mode shapes results	**62**
Figure 4.16 Discretization, Visualisation and mode shapes results	**63**
Figure 4.17 Discretization, Visualisation and mode shapes results	**63**
Figure 5.1: Probable non-linear buckling load-displacement behaviour	**65**
Figure 5.2: Graphical example of the modified RIKS method	**67**
Figure 5.3: Importing the node file command in the Buckle step	**71**
Figure 5.4: Choosing Static, RIKS Step	**71**
Figure 5.5: Adding Imperfection commands in input file	**72**
Figure 5.6: Executing the linear buckling analysis	**72**
Figure 5.7: Copy the model	**73**
Figure 5.8: Material properties	**73**
Figure 5.9: Performing RIKS analysis	**73**
Figure 5.10: Introducing the imperfection as per EC3 (1/1000)	**73**
Figure 5.11: Deformed shape at ultimate increment	**73**
Figure 5.12: ultimate increment for single circular opening	**75**
Figure 5.13: Load-deflection curve	**75**
Figure 5.14 ultimate increment for single square opening	**75**
Figure 5.15 Load-deflection curve	**75**
Figure 5.16 ultimate increment for single rectangular opening	**75**
Figure 5.17 Load-deflection curve	**75**
Figure 5.18 ultimate increment for multi-circular opening	**76**
Figure 5.19 Load-deflection curve	**76**
Figure 5.20 ultimate increment for multi- rectangular opening	**76**
Figure 5.21 Load-deflection curve	**76**

Abstract

Web-opening beams (WOB) are commonly used in construction due to their several advantages. However, the shape and number of holes significantly impact the general behaviour of such structures. This dissertation is subdivided into main two parts. The first part, from chapters 1 to 3 is dealing with the necessary background on WOB steel structures with an updated literature review (2025) and the different aspects of behaviours of such structures including their potential modes of failure, buckling strength. The second part of this work concerns the assessment of the of web-opening on the linear and nonlinear torsional buckling behaviour, while chapter 4 is devoted to linear buckling analysis results and discussion whereas chapter 5 concerns the nonlinear post-buckling analysis results and discussion. Furthermore, chapters 4 and 5 contain the necessary theoretical background for linear and nonlinear buckling F.E. analysis and the way how to perform each type of analysis using software. Also, a detailed study was carried out taking into account several parameters: shape and number of openings; the location of the applied load for linear buckling analysis adding to the sensitivity to imperfection and plastic characteristics in the nonlinear post-buckling analysis. To achieve this goal, dozens of three-dimensional models were built-up in ABAQUS. As detailed in Chapter 4, the numerical models of WOB were validated against the case of a solid beam (LTBeam) and subsequently utilised in a parametric study. From the results of elastic linear buckling, it was found that the strength of a perforated beam to LTB is alternated by the presence of the holes associated to the location of the applied load in the cross section where the top flange being the worst case with a higher stiffness reduction. Furthermore, the number of holes (single or multi), the geometrical shapes (circular, square and rectangular), and the sizes of perforations is seen to be decisive parameters. This explains the significant drop in Mcr values observed in certain cases with multiple rectangular perforations being the weakest configurations. The results showed that a reduction of 1% to 6 % for single web opening to 9% to 24 % reduced the flexural capacity against LTB. RIKS method implanted in Abaqus has been used for nonlinear post-buckling analysis. Except from the first model dealing with a single circular opening which gives an acceptable load- deflection including linear and nonlinear branches with a clear post-buckling behaviour. The remaining models including single and multi-hole fail to give satisfactory results though the same steps were followed. The model seems to stop running when it's the beam pass through the bifurcation point about a deflection of 10 mm. Despite the efforts made to overcome this problem for more than four weeks by changing the number of increments, LPF, plastic characteristics, transverse maximum displacement the obtained curves remain the same with different values for Pcr.

Keywords: WOB, LTB, linear and nonlinear buckling, post-buckling, RIKS method, mode shapes; imperfections, Mcr, ABAQUS.

Résumé

Les poutres à ouverture d'âme sont couramment utilisées dans la construction en raison de leurs nombreux avantages. Cependant, la forme et le nombre de trous influencent considérablement le comportement général de ces structures. Ce mémoire est divisé en deux parties principales. La première partie (chapitres 1-3) traite des connaissances générales sur les structures en acier avec ouvertures dans l'âme, en même temps qu'une revue bibliographique mise à jour (2025), et les différents aspects du comportement de ces structures, notamment leurs modes de rupture et leurs flambement. La deuxième partie étudie l'impact de la présence d'ouvertures dans les âmes sur le comportement au déversement linéaire et non linéaire. Le chapitre 4 présente les résultats et la discussion de l'analyse linéaire, et l'analyse et les résultats ainsi que la discussion du déversement non linéaire sont donnés dans le chapitre 5. De plus, les chapitres 4 et 5 présentent les bases théoriques nécessaires à l'analyse du déversement linéaire et non linéaire, ainsi que la manière de réaliser chaque type d'analyse en utilisant ABAQUS. Une étude détaillée a également été réalisée en tenant compte de plusieurs paramètres : la forme et le nombre d'ouvertures ; la localisation de la charge appliquée pour l'analyse et la sensibilité aux imperfections et aux caractéristiques plastiques de l'analyse pour l'analyse non linéaire et post-flambement. Pour atteindre cet objectif, des dizaines de modèles tridimensionnels ont été créés dans ABAQUS. Comme détaillé au chapitre 4, les modèles numériques de WOB ont été validés dans le cas d'une poutre pleine (LTBeam) puis utilisés dans une étude paramétrique. Les résultats du flambement linéaire élastique ont montré que la résistance d'une poutre perforée au déversement est influencée par la présence de trous dans l'âme associés au niveau d'application de la charge transversale, la semelle supérieure étant le cas le plus défavorable, avec une diminution de résistance plus importante. De plus, le nombre (simple ou multiple), les formes géométriques (circulaires, carrées et rectangulaires) et la taille des perforations sont des paramètres déterminants. Ceci explique la baisse significative des valeurs M_{cr} observée dans certains cas, les perforations rectangulaires multiples étant les configurations les plus fragiles. Les résultats ont montré qu'une réduction de 1 % à 6 % pour une ouverture d'âme unique à 9 % à 24 % réduisait la capacité de flexion contre la déformation élastique. La méthode RIKS, intégrée à Abaqus, a été utilisée pour l'analyse post-flambement non linéaire. À l'exception du premier modèle, portant sur une seule ouverture circulaire, qui donne une charge-déformation acceptable, incluant des branches linéaires et non linéaires, avec un comportement post-flambement clair, les autres modèles, incluant des trous simples et multiples, ne donnent pas de résultats satisfaisants, bien que les mêmes étapes aient été suivies. Le modèle semble s'arrêter lorsque la poutre passe par le point de bifurcation pour une déplacement d'environ 10 mm. Malgré les efforts déployés pendant plus de quatre semaines pour résoudre ce problème en modifiant le nombre d'incréments, le facteur de puissance linéaire (LPF), les caractéristiques plastiques et le déplacement transversal maximal, les courbes obtenues restent inchangées avec différentes valeurs pour P_{cr}.

Mots-clés : poutres alvéolaires, déformation élastique, déversement linéaire et non linéaire, post-flambement, méthode de RIKS, formes modales ; imperfection, M_{cr}, ABAQUS.

ملخص

تُستخدم عوارض فتحات الويب (WOB) بشكل شائع في البناء نظرًا لمزاياها العديدة. ومع ذلك، يؤثر شكل وعدد الثقوب بشكل كبير على السلوك العام لهذه الهياكل. تنقسم هذه الرسالة إلى جزأين رئيسيين. يتناول الجزء الأول، من الفصل الأول من 1 إلى 3، الخلفية اللازمة عن الهياكل الفولاذية ذات الفتحات الفولاذية مع مراجعة الأدبيات المحدثة (2025) والجوانب المختلفة لسلوكيات هذه الهياكل بما في ذلك أنماط فشلها واستجابة الالتواء. ويتعلق الجزء الثاني بدراسة تأثير وجود الفتحة في الشبكات على سلوك الالتواء الخطي وغير الخطي، أما الفصل الرابع فقد خُصص لنتائج التحليل الخطي والمناقشة، بينما يتعلق الفصل الخامس بنتائج التحليل غير الخطي بعد الالتواء والمناقشة. علاوةً على ذلك، يحتوي الفصلان 4 و5 على الخلفية النظرية اللازمة لتحليل الالتواء الخطي وغير الخطي .F.E وطريقة إجراء كل نوع من التحليل باستخدام البرمجيات. كما تم إجراء دراسة مفصلة مع الأخذ بعين الاعتبار عدة معايير: شكل وعدد الفتحات؛ وموقع الحمل المطبق لتحليل الالتواء الخطي إضافة إلى الحساسية للعيوب والخصائص البلاستيكية في التحليل غير الخطي بعد الالتواء. ولتحقيق هذا الهدف، تم بناء العشرات من النماذج ثلاثية الأبعاد فيABAQUS . كما هو مفصّل في الفصل 4، تم التحقق من صحة النماذج العددية لـ WOB في حالة العارضة الصلبة (LTBeam) واستخدمت بعد ذلك في دراسة بارامترية. من نتائج الالتواء الخطي المرن، وُجد أن قوة العارضة المثقوبة إلى LTB تتناوب مع وجود القطع المرتبط بمستوى تطبيق الحمل المستعرض، حيث تكون الحافة العلوية هي الحالة الأسوأ مع تناقص أعلى في المقاومة. علاوة على ذلك، يُلاحظ أن العدد (فردي أو متعدد)، والأشكال الهندسية (دائرية ومربعة ومستطيلة)، وأحجام الثقوب هي معايير حاسمة. وهذا ما يفسر الانخفاض الكبير في قيم Mcr التي لوحظت في بعض الحالات مع وجود ثقوب مستطيلة متعددة هي أضعف التكوينات. أظهرت النتائج أن الانخفاض من 1% إلى 6% للفتحة الواحدة إلى 9% إلى 24% يقلل من قدرة الانثناء ضد ثقوب الشدات المستطيلة. استُخدمت طريقة RIKS المزروعة في Abaqus لتحليل ما بعد الانحناء غير الخطي. باستثناء النموذج الأول الذي يتعامل مع فتحة دائرية واحدة والذي يعطي انحرافًا مقبولًا للحمل - الانحراف بما في ذلك الفروع الخطية وغير الخطية مع سلوك واضح بعد الانحناء. فشلت النماذج المتبقية بما في ذلك النماذج أحادية الفتحة ومتعددة الفتحات في إعطاء نتائج مرضية على الرغم من اتباع نفس الخطوات. يبدو أن النموذج يتوقف عن العمل عندما تمر الحزمة من خلال نقطة التشعب حول انحراف 10 مم. على الرغم من الجهود المبذولة للتغلب على هذه المشكلة لأكثر من أربعة أسابيع من خلال تغيير عدد الزيادات، وعامل التثبيت المنخفض، وخصائص اللدائن، والإزاحة القصوى العرضية، فإن المنحنيات التي تم الحصول عليها تظل كما هي مع اختلاف قيم Pcr.

الكلمات المفتاحيةWOB : LTB، التواء خطي وغير خطي، التواء ما بعد الالتواء، طريقةRIKS ، أشكال الأنماط؛ العيوب، Mcr، ABAQUS

TABLE OF CONTENTS

Acknowledgements	/
Dedication	/
List of Symbols	V
List of Tables	VII
List of Figures	VIII
Abstract	A
General Introduction	H
CHAPTER 1: Steel Beams with Openings	
1.1 Introduction	1
1.2 Origin of Castellated Beams	1
1.3 Formation of Openings	1
1.4 Components of a Typical Castellated Beam	2
1.5 Structural Elements with Web Openings	3
1.6 Advantages of Beams with Openings (BWO)	4
1.7 Drawbacks of BWO	5
1.8 Application Fields	5
1.9 Opening Shapes	6
1.9.1 Common types of WO with and without reinforcement	7
1.9.2 Advanced types	9
1.9.3 Geometry	10
1.10 Manufacturing	11
1.11 Behaviour of Castellated Steel Beams	13
Chapter 2: Lateral Distortional Buckling of Web Openings in Steel Structures	
2.1 General	15
2.2 Overview of Research on Distortion	16
2.3 Classical Lateral Torsional Buckling Solution	18
2.4 Standard Design Provisions	19
2.5 Analysis of Distortional Dimensional Effects	20
2.6 Literature Review	22
2.6.1 Lateral Torsional Buckling	23
2.6.2 Lateral distortional buckling	23
2.6.3 Web-post buckling and other failure modes	24
2.6.4 particular studies on cellular steel beams	25
Chapter 3: Behaviour of Steel Beams with Web Openings	
3.1 Introduction	26
3.2 General Behaviour of Web-Opening Beams	26
3.2.1 Effect of opening on force distribution	26
3.2.2 Failure mechanisms due to web openings	27
3.3 Openings without Stiffeners	28

3.3.1 Early Studies on Castellated Beams	28
3.3.2 Influence of opening shapes on structural performance	28
3.3.3 Numerical and experimental studies on beams with web opening	29
3.4 Openings with Stiffeners	30
3.4.1 Influence of stiffeners on beam stability	30
3.4.2 Types of stiffeners and their effectiveness	30
3.4.3 Experimental Studies on Stiffened Beams	32
3.4.4 Summary of the above literature review	32
3.5 Failure Modes and Structural Analysis	32
3.5.1 General	32
3.5.2 Vierendeel Bending	33
3.5.3 Shear in the perforated section	35
3.5.4 Shear Buckling of the Web Panel	36
3.5.5 Buckling of the Web Post	37
3.5.6 Lateral -torsional buckling	38
3.5.7 Additional Deflection	39
Chapter 4: NUMERICAL LINEAR EIGEN FINITE ELEMENT ANALYSIS FOR LTB : CASES STUDIED	
4.1 Finite element method and its concepts	41
4.1.1 General	41
4.1.2 Steps in Finite Element Analysis	41
4.2 Buckling of Members	42
4.2.1 General	42
4.2.2 Lateral torsional buckling of bending members	42
4.3 Finite Element Analysis of Buckling Problems	43
4.3.1 Introduction	43
4.3.2 Performing Eigenvalue buckling analysis	43
4.3.3 Assumptions and methods of analysis	44

4.3.4 Procedure of solving linear eigen buckling problem (ABAQUS)	**45**
4.4 Introduction Software used in this dissertation	**46**
4.4.1 LTBEAM	**46**
4.4.2 ABAQUS Software for Elastic and Inelastic Buckling	**49**
4.5 Linear Buckling Analysis (ABAQUS)	**52**
4.5.1 General	**52**
4.5.2 Steps to perform a linear buckling analysis (LBA)	**52**
4.6 Studied cases	**56**
4.6.1 General features of the numerical models	**56**
4.7 Overall discussion	**58**
4.7.1 General	**58**
4.7.2 Validation of the model	**58**
4.7.3 Models with perforated web	**59**
4.8 Conclusion	**63**
Chapter 5: NONLINEAR NUMERICAL BUCKLING MODELLING OF WEB -OPENINGS SECTIONS: STUDIED CASES	
5.1 Introduction to Nonlinear Buckling Behaviour	**64**
5.2 Nonlinear LTB post buckling analysis	**64**
5.3 Imperfection sensitivity of thin structures	**65**
5.4 Over-all on nonlinear post-buckling using Abaqus.	**66**
5.4.1 Unstable Behaviour of a thin structure	**66**
5.4.2 Nonlinear buckling using RIKS method implanted in ABAQUS	**67**
5.4.3 Load Proportionally Factor (LPF)	**68**
5.5 Practical Step by step procedure for nonlinear buckling in ABAQUS	**68**
5.5.1 Input file template	**69**
5.5.2 Demonstration	**72**
5.6 Studied cases	**74**

GENERAL INTRODUCTION

General on the dissertation

Nowadays, the use web openings in I-section steel beams has become increasingly common and can be observed in various civil engineering structures. They are used to allow the passageway of services within the beam and can also be so supportive and essential from an economic point of view. Steel beams with web openings also gives a significant solution when height constraints are imposed on multi-storey buildings when considering design regulations and economic reflexions. However, while the openings can reduce material usage, web openings might lead to a notable reduction in the overall stiffness load-carrying capacity of beams, and also can introduce other failure modes. Section having web openings can bring local instability or yielding due to insufficient shear force transfer across holes leading to the formation of plastic hinges making a Vierendeel mechanism possible. More advanced geometric forms are used as explained in Chapter1. It is well-known that beams must be designed to have the required against lateral-torsional buckling. The design procedure defined in Eurocode 3 is based on the evaluation of the critical bending moment value which provides the slenderness value, needed to calculate the reduction factor used for the design verification. Also, a parametric study, using ABAQUS software, is presented in this dissertation to study on the linear and nonlinear LTB behaviour of A numerical a parametric analysis carried out on unrestrained simply supported steel web opening steel structures the influence of varying the shape of openings in order to assess the elastic (eigen) and nonlinear buckling capacity using Abaqus software capabilities. The results were very satisfactory for linear eigen buckling analysis notably with the validation of the model and give logical values for M_{cr} expressing the influence of the geometric hole and their number. Some problems have risen when the nonlinear assessment begun. Despite the fact that the procedure to perform RIKS analysis was correct, some of the results seem to be logical. Although the temptation to understand the problem by dozen building-up modelling the same results are exhibited. Conclusions are drawn to end-up the work with some recommendations for future works.

Objective of the work described in this dissertation:

The main objective of the work described herein was to a deep understanding of the linear and nonlinear behaviours of steel with web-opening beams and the impact of LTB on the carrying capacity of such structures. Despite the fact that the nonlinear buckling analysis was not satisfactory executed, I consider that I have achieved a good insight in this advanced topic. Three-dimensional modelling with the imperfection sensitivity to take into account of geometric nonlinearity was a good experience for me.

Methodology followed in preparation of this dissertation:

This dissertation has been sub-divided into five chapters as follows:

General Introduction: A general introduction is provided giving a brief information on the work undertaken in this study and its objectives.

Chapter 1: gives a general presentation of steel beams with web opening as well as their structural compounds, common and advanced shapes, their process of manufacturing fabrication and the general behaviour and their field of application.

Chapter 2: This chapter deals with the Lateral Distortional Buckling concept of web opening in steel structures, presenting the essential of the classical Lateral Torsional Buckling theory and effects. Also, standard design provisions are provided with an updated literature review.

Chapter 3: In this chapter, the general behaviour of web-opening of steel structures is given. The effect of reinforcing the holes by means of stiffeners and its impact on the behaviour is fully discussed. Modes of failure are presented and debated.

Chapter 4: Representing the main part of this dissertation. It treats the linear eigen buckling analysis by the cases studied modelling and discussions. Besides, it presents the concepts of FEA and its solution for buckling problems. Some conclusions were drawn.

Chapter 5: This chapter deals with a numerical a parametric analysis carried out on unrestrained simply supported steel web opening steel structures in order to assess the elastic (eigen) and nonlinear buckling capacity using Abaqus software capabilities. An introduction to the nonlinear buckling post-buckling analysis background is given. The procedure of performing a full nonlinear post-buckling analysis taking into account geometric and material nonlinearity is carried out using ABAQUS is provided. The results of some studied cases will be presented.

Conclusion and recommendations for future works

CHAPTER1:

Steel beams with openings

1.1 Introduction

In modern architecture, various solutions have been developed to reduce costs while enhancing the efficiency of steel structures. Over the past few decades, extensive theoretical, numerical, and experimental research has been conducted on the structural behaviour of steel beams with web openings of different shapes, demonstrating their effectiveness in improving performance without increasing weight. While the use of cellular columns is less common, examples can be found in the literature, yet this topic has received limited research attention [1]. At the same time, certain engineering applications, such as industrial facilities and multi-stories buildings, require passageways for pipelines and ventilation ducts, prompting major construction companies to seek innovative solutions. Among these advancements, castellated beams have emerged as an effective option, providing increased stiffness without additional weight, reducing costs, and enhancing aesthetic appeal, making them widely used in modern projects According to [2].

1.2 Origin of castellated beams

The Castellated beam name is derived from the Latin word "castellatus" meaning "built like a castle having regular openings in walls like a castle." These beams were introduced to improve the depth and strength of the beam without adding more material or weight.

Due to shortage of steel immediately after WWII, engineers discovered that castellated beams were cheap to build and had an excellent strength-to-weight ratio. As a result, castellated beams have been the preferred building solution since the 1950s and were commonly used in Europe to decrease the cost of steel structures due to the low ratio of labour cost to material cost. Most of the material presented in subsequent sections is taken from [1]

1.3 Formation of openings

The BWO can be formed both by providing simple cuttings in the web to provide for passage of service lines in a building. These cut-outs may have different geometric forms: rectangular or circular. The choice of the geometric form is depending on service requirements as well aesthetic requirements. These opening can be equipped with or without stiffeners according to the structural strength requirements. However castellated beams are those which are formed by cutting the existing rolled sections in such a way as described in the figure below (Figure 1.1) to obtain greater depth and high capacity of the final section without increasing the overall weight of the beam itself. The four stages or sequences of formation of typical castellated beam is as shown below in Figure. 1.1 taken from

(Picture Courtesy: AISC Journal). The final product is a castellated beam with Hexagonal castellations with increased depth compared to the original sections which ensures better section modulus and strength.

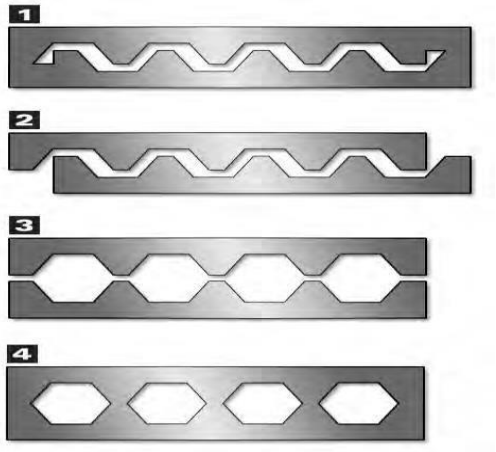


Figure1.1 Necessary stages for forming a castellated beam [1]

1.4 Components of a typical a castellated beam

The basic structural components of the castellated beams are as shown in Figure.1.2 below and these components are the ones which need to be sufficiently strong individually. The terminology used in this dissertation to denote each part of concerning the web-opening steel sections is as follows:

- **Web post**: signifies the cross-section of the castellated beam where the section is a solid cross- section.
- **Castellation**: denotes the area of the castellated beam where the web has been expanded by the formation of hole section though the web.
- **Throat width**: commonly represents the length of the horizontal hole operated in the beam.
- **Throat depth**: represents the height of the part of the web that links to the flanges in order to form the tee section.
- **Top tee**: means the section formed at the top of castellation by the flange and web above the cuts.
- **Bottom tee**: denotes the inverted Tee section formed at the bottom of castellation by the flange and web below the cuts.

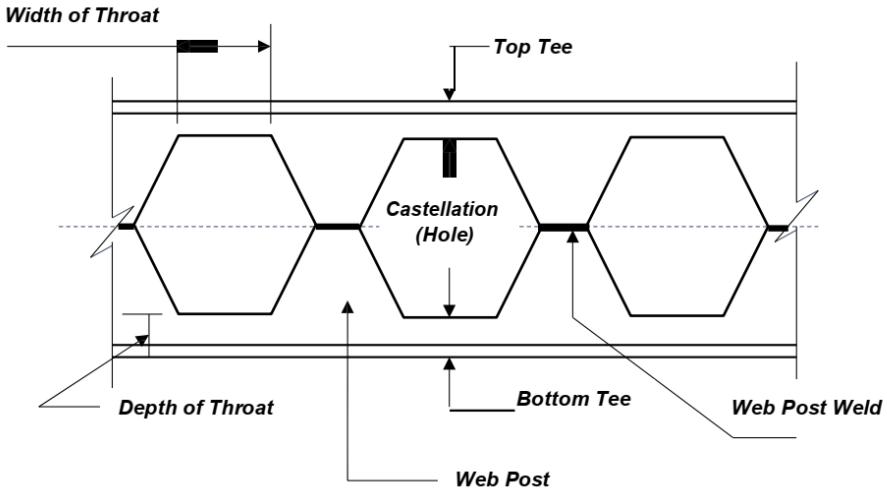


Figure 1.2 Different structural elements of a castellated beam [1]

1.5 Structural elements with web opening

According to [2], an opening web steel beam is an I-shaped beam section with diverse shape opening that is hexagonal, rectangular, circular, diamond or oval in shape. The use of WOB has resulted in much longer span. Their popularity has also increased because due to an architectural emphasis on longer spans which characterise modern constructions. In the United States and Canada during the 60's ,70's and 80s studies on different web opening configurations were achieved considering different shapes: circular, square and rectangular considering both concentric, and eccentric openings for both composite and non-composite steel beams. Nowadays, in most cases, the design of floor beams with web openings is carried out identifying the composite action between the steel beam and the concrete slab on top of it [3].

Some simplified rules for opening design were suggested by the British Standard (BSI, 2000) and the Canadian Standard (CSA, 2001). These guidelines are provided in order to avoid the weakening of such beam. Because these rules cover a wide variety of options, and, so, they are very conservative and, in general, with restriction to operate the openings at the middle, third of the beam depth and to the two located at the central quarters of the beam span length.



Figure1.3 Example of various web opening shapes in floor beams [2].

1.6 Advantages of BWO

BWO beams have several advantages a number of these advantages are given in the following [1, 2]:

- Castellated beams the use of BWO significantly improve the design. These benefits include:
  - The ability to spread the length of the beam reducing the need for supplementary columns.
  - Castellated beams improve the aesthetic appearance of the constructions structure and permit more natural light to enter the construction.
- The use o BWO reduces the floor-to-floor height which impacts the ventilation canals, heating and cooling schemes, electrical and data communication arrangements, fire protection equipment, and composition cables which can pass inside of the web openings.
- Carrying capacity for higher bending moment with no need for additional steel.
- Lower, faster and easier installation maintenance with less compared to other structures due essentially to the longer span, and easier handling due to the lighter weight.
- BWO beams have a high stiffness-to-weight ratio which lead to a reduction of effect of vibrations.
- BWO can be designed asymmetrically to undergo more transverse loads.
- BWO are more economical compared to other types of structures, leading to a decrease in the overall cost of the construction.

1.7 Drawbacks of BWO

The main disadvantage of BWO is the increased cost of manufacture due to the cutting and welding required to form such structures [4-5]. It must be mentioned that the size limitations for the holes in BWO could require adjustments to accommodate larger services [6]. Other disadvantages and areas of concern include:

- BWO are subjected to six major modes of failure:
- Vierendeel mechanism.
- Distortional or Lateral-torsional buckling of the web- post.
- Lateral-torsional buckling of the whole beam.
- Web post local buckling
- . Formation of a plastic flexure mechanism

1.8 Application fields

According to [2]. open web expanded steel beams were firstly used in structures during World War II to reduce the cost of steel structures. The use of BWO became common in the 90's. The main concern in this type of structure is the increasing of the stiffness and strength of the original beam has been the main purpose of the selection of these beams from designers.

The ability to use more longer and lighter spans makes very few members required for a given system naturally saving construction costs. Parking garages, industrial and warehouse facilities, office buildings, schools, and hospitals are structures. The practical use of such structures can be found when long open space is needed [7].

The Westok brochure14 recommends that BWO are most economical when used in the case of long span secondary members. Furthermore, BWO beams are frequently used in floor support systems, accommodating the constructions systems (heating, ventilation, air conditioning, etc.) along with the structural support within the ceiling spaces, [8]



Figure1.4 Examples for application fields of BWO:

(a) (Left)Service incorporation with ceiling attached to structure;

(b) (Right) Curved BWO roof structure, adapted from [8]

1.9 Opening shapes

BWO are generally classified depending on type or configuration shape of perforation made in the web of the beam; hence the shape of the web openings will depend upon the designer's choice and the opening purpose, however Steel members can be equipped with single or multiple web openings, which can take different shapes. When these openings are circular and regularly spaced, the members are selected as cellular. Also, depending on the fabrication procedure other opening shapes are possible :square, rectangular, hexagonal and octagonal shapes.[3] but can include also irregular openings that are employed under certain circumstances where a adjustment is necessary, Owing to the rapid development of fabrication technology, more complex profiles of the BWO have become possible including elongated openings, tapered sections and curved beams.[9]



Figure1.5 Example of roof opening's beam applications

1.9.1 Common types of WOB with and without reinforcement

- Web with centrally placed hole without reinforcement

a-web with hexagonal



Figure1.6 Example of castellated beams [2]

b- Web with centrally placed circular hole



Figure1.7 Example of cellular beams [2]

c- Web with centrally placed rectangular hole:



Figure1.8 Beam with rectangular shape opening [2]

- Web with centrally placed hole with reinforcement

Reinforcement will be necessary when a WOB fails to perform satisfactorily because of high shear areas in the vicinity of the supports. Reinforce one or more openings and buckling of a web-post can be avoided by adding two-part studs or a simple flat plate.

a-Web having a centrally placed circular hole with reinforcement:



Figure1.9 cellular beam with circular reinforcements [2]

b-Web having centrally placed rectangular hole with reinforcement



Figure1.10 rectangular shape with large reinforcement [2]

1.9.2 Advanced types

- **Ellipse web opening**

New studies were carried out and focused on the optimization of new elliptically based web opening shapes which improve the structural behaviour of the perforated beams as well as leading to economic design in terms of both manufacture and usage,

An general study of several standard and non-standard web opening shapes it was revealed that perforated beams with vertical and inclined classic elliptical web opening behave more efficiently compared to perforated beams with conventional shapes specially in terms of stress distribution and local deflection.

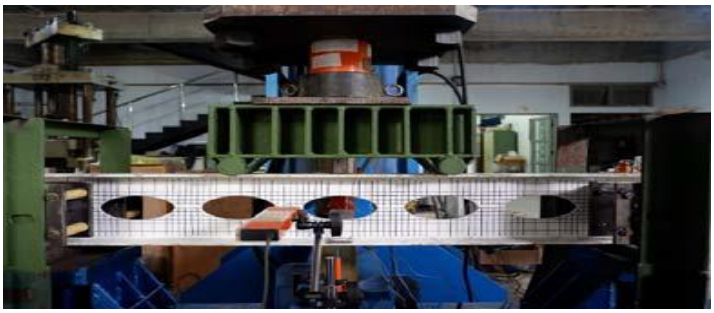


Figure1.11 Ellipse openings. [2]

- **Sinusoidal web opening**

This shape gives a new architectural dimension in an environmentally friendly approach, the ANGELINA beam which are manufactured from H or I beam, by cutting through the web along a single sinusoidal line. The two T sections are off-set and welded to each other ending in a beam with one and a half times deeper than the original profile.



Figure1.12 Angelina beams [2]

1.9.3 Geometry

Depending on the design for a assumed section numerous opening combinations, sizes, and spacings can be applied, [8]. Table 1.1 shows the ranges of dimensions difference changing according to their applications field and the objective. These dimensions are represented by the diameter $a0$ of the hole openings, the distance S between holes, the height h of the profile of the solid beam that gives increase to the BWO, and the final height H of the BWO.

Table 1.1 Variation of geometric dimensions of cellular beams according to application and objective, [8].

Applications	Objective	a_0	S	H
Roofing, footbridges, and wide-span purlins	Optimization of the height/weight ratio	$1.0-1.3h$	$1.1-1.3a_0$	$1.4-1.6h$
Floors, parking structures and offshore structures	Optimization of the load/weight ratio	$0.8-1.1h$	$1.2-1.7a_0$	$1.3-1.4h$

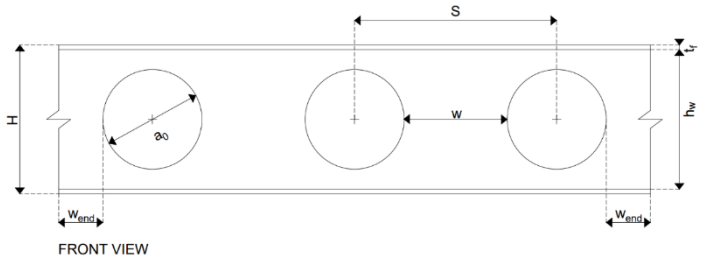


Figure1.13 Geometric dimensions of the BWO [8]

According to [2] The geometry and dimensions of a perforated section according to the Eurocodes (annex N) are covered as bellow and are defined:

- For rectangular opening: d0, and length a0;
- For Circular opening: radius r0;
- For Extended circular opening: depth d0, and end radius r0;
- For Hexagonal opening: depth d_0 and lengtha_0 and the tee length a_{0eff};
- For Octagonal opening: depth d0 and length a0, the tee length a0 eff, and the extension plate dimension d0.

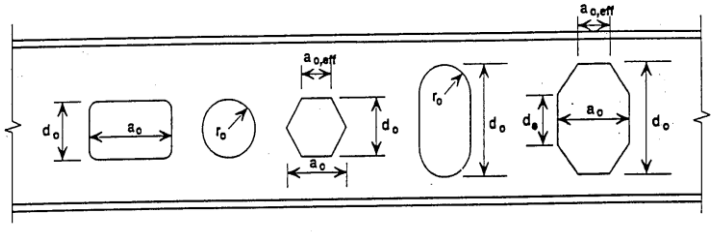


Figure1.14 Details of the geometry of the openings. [2]

Cross section of perforates beam

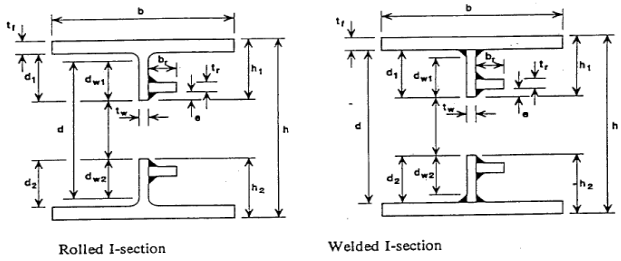


Figure1.15 Profile geometry of WOB section [2]

1.10 Manufacturing

The manufacturing process of beams with web openings is a decisive factor as it affects both the total cost and the structural future behaviour of the final product. BWO are produced by means of a profile-cutting method offering several advantages with a procedure to optimized and minimize costs. BWO are manufactured by a single zigzag cut, followed by gathering the two halves and welding them back together [7].

The height of a cellular beam increases by 40% to 60% times are compared to the parent section, making it more economical when subjected to strong-axis bending [10]. Moreover, circular openings enhance the overall beam depth, moment of inertia, and section modulus though reduction of the beam's overall weight, making cellular beams more efficient and economical solution.[11]. Furthermore, perforated beams can be manufactured using different methods, including:

- Fabricating a built-up section: Shaped by welding three plates to create an I-section, with openings introduced either before or after manufacture.
- Cutting and reassembling a hot-rolled section:

-

-



Figure1.16 Manufacture process for perforated steel beams. [2]

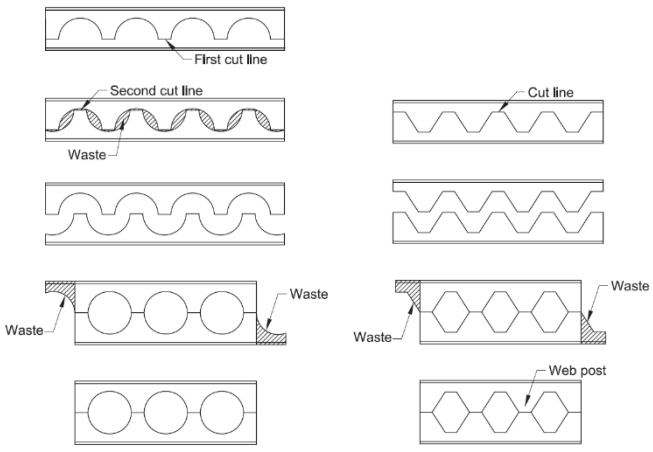


Figure1.17 Fabrication process: (a) cellular beams; (b) castellated beams, adapted from[8]

1.11 Behaviour of castellated steel beams

Experimental studies on castellated steel beams have identified six main modes of failure, closely associated with the geometry of the overall beam, web slenderness, aperture size, type of loading, boundary conditions, aperture position and aperture stiffening method. A distinction can be made between local failure modes at openings and global failure modes [12][13].

- **Local failure modes**

Local modes involve local sections around the opening and include:

- Vierendeel bending: caused by shear transfer around the opening it corresponds to a local bending of tee sections.
- Intermediate column buckling: as a result of horizontal shear or direct compression due to point loading [14].
- Intermediate post weld failure: associated with horizontal post shear [15][16].

- **Global modes of failure**

Global modes affect the whole beam and include:

- Global bending: occurs when the critical opening is located in a pure bending zone, which leads to a plasticization of the top and bottom members under tension or compression.
- Global shear: is located in a high-shear zone of short length in the opening [17].
- Global torsional buckling: the main mode of failure occurs and reduce their torsional stiffness [13].
- The presence of large openings in the web of a beam generates specific mechanical behaviours compared to solid web beams. Because of the opening, global forces are transformed into local forces in the top and bottom chords. The global moment in the section is translated into a pair of local normal forces, while shear forces are distributed between the two members. This distribution of forces is illustrated in Figure I-10. Depending on this distribution, the different modes of failure that can occur are:

  - Plasticization under normal load
  - Shearing of the web
  - Vierendeel mechanism.
  - Buckling in the plane of the web.
  - Shear buckling [18-19-20].

CHAPTER 2:

LATERAL DISTORTIONAL BUCKLING OF WEB OPENING IN STEEL STRUCTURES

2.1 General

It is well known that buckling phenomenon are critical issues in steel structure design, as it can lead to severe structural failure. Among these phenomena, Lateral Torsional Buckling (LTB) is one of the most common forms of instability, particularly for the case of slender I-sections under bending loading, for which instability behaviour of the structural element is complex. Buckling can be classified into two main types: local buckling, which involves the loss of stability in compressed plates such as the flange and web, and global lateral torsional buckling, which leads to a loss of equilibrium in the primary bending plane, causing lateral displacement combined with twisting. Both stocky and slender members are susceptible to this form of instability.

According to [21], the AISC, LTB is defined as a buckling mode in which a flexural member deflects out of its bending plane while simultaneously twisting about its shear centre. As illustrated in Fig. 2.1, before loading, the beam's cross-section is in its initial position. Upon loading, it experiences transverse deflection w, and if the applied load reaches a critical magnitude, the beam experiences lateral deflection along with a twist by an angle ϕ about the shear centre. At this stage, structure is declared failed, by losing its aptitude to resist added forces. Despite the significance of LTB in structural design, closed-form classical solutions are available only for limited cases.

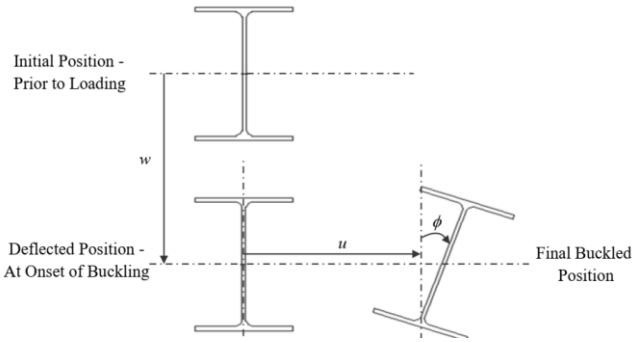


Figure 2.1 Cross-section during lateral torsional buckling at the initial configuration, at onset of buckling, and in the final position [21].

2.2 General on research works on Distortion phenomenon

Once studying intermediate-length members, two buckling modes which are lateral-torsional buckling and local buckling will interrelate and lead to a lateral-distortional

buckling (LDB), which is characterised by the apparition of an interaction between lateral deflection, twist, and cross-sectional changes due to web distortion.

Buckling of steel element under bending is treated as either lateral-torsional buckling or local buckling as separate phenomena. However, researchers recognized early that these modes may interact. When both modes have the same half-wave-length, the phenomenon of distortional buckling occurs which is characterized by a simultaneous lateral deflections and cross-sectional distortions at the bifurcation of equilibrium. This type of buckling can generally be analysed using linear eigenproblem analysis [22]. The first studies on LDB were treated [23], where the authors noticed that the general distribution of stresses and of displacements were meaningfully modified by web slenderness. Later, it was verified via finite element modelling that LDB occurs mainly for intermediate lengths of beams with slender web section. However, the author accessed only beams which undergo uniform bending [24]. On the other hand, authors in [25] considered the effects of loading on stabilising and destabilising. The authors mentioned dissimilar behaviour as a function of load positioning and verified that critical moment values in LDB are always lower than LTB's. Using a plate buckling distortional solution, the authors proposed the buckling characteristic equation of wide flange sections.

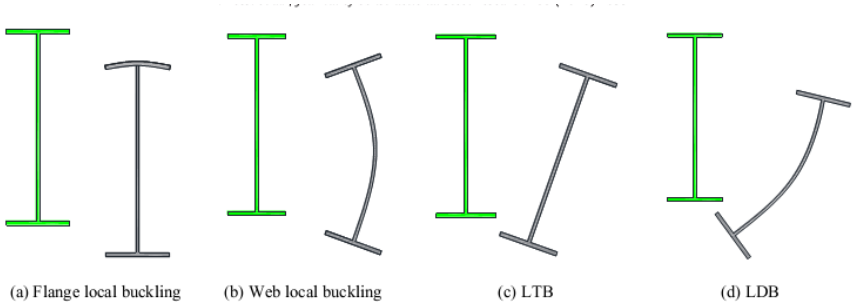


Figure 2.2 Buckling Modes in I Beams with a focus on distortion [25]

Different from the LTB and local buckling, and due to web distortion (Fig. 2.2.d), the LDB of I-beams is characterized by simultaneous lateral deflection, twist and cross-sectional as studied by authors [26–33]. Although there is consensus on the kind of buckling modes, there is no precise definition of LDB since the I-section deformation patterns present characteristics a combination of buckling modes [26].

The web distortion introduces effects not found in LTB. This phenomenon is responsible for the reduction of the cross section torsional stiffness; the parallel flanges may have different angles of twist rotation during buckling, and the originally doubled symmetrical I-section becomes un-symmetric during LDB [34]. This results in a reduction of the resistance of these structural elements. For all these reasons, the strength of the beam to

LDB becomes lower than the resistance to LTB, and it is significant and needs to be considered in design [25–40]. For all these reasons, the strength of the beam to LDB becomes lower than the resistance to LTB, and it is significant and needs to be considered in design [25–40].

The numerical accurate modelling of distortional buckling was not possible until the arrival of digital computers. So while many lateral-torsional and local buckling problems were solved earlier this century, distortional buckling problems have generally been solvable in the recent decades. Apart from early work, [29-31], attempt have been made to study distortional buckling the last decade or so, mainly for thin-walled sections that have been fabricated recently by means of modern and efficient techniques.

In Cellular beams cases which are appropriate for large spans with relatively small loads or for conditions where strain dictates dimensioning.

Castellated beams may experience a LTB before they can reach to their ultimate limit state. Recent indication explains that due to applying transverse loads on the major axis of the BWO, the section is affected by compression and tension stresses. The combinations of these stresses are capable to produce a lateral-torsional buckling as mentioned [25].

Imperfections in BWO result from a lack of straightness during fabrication of rolled profiles which can be represented numerically by an initial curvature. Additionally, the physical imperfections of rolled profiles result from the appearance of residual stresses. The condition that creates residual stresses in steel is the result of thermal and mechanical industrial processes. In the study of this kind of steel members, numerical linear and nonlinear analyses can be performed by using Finite Element Method software (Abaqus, Ansys etc.). During the simulations, through nonlinear geometric and physical analyses, geometric imperfections can vary, where lateral torsional buckling in cellular beams was considered as a function of the unrestrained length. In the boundary, conditions were restrained displacements in 3 D modelling the Cartesian axis X, Y, Z and rotation about X-axis, thus simulating the fork support (simply supported beam). The results from the numerical analyses were compared with the calculation procedures, which verified that the results were significant.

2.3 Classical theory for Lateral Torsional Buckling Solution

According to [21], the classic theory of the lateral torsional buckling capacity of a beam considers the case of a doubly symmetric wide flange section, various structural steel design standards utilise, the classical closed form expression of the critical moment *Mu* for a simply supported beam under uniform moments derived by [2,1]:

$$Mu=\frac{\pi}{lu}\sqrt{EIyGJ+(\frac{\pi E}{LU})2IyCw} \qquad 2.1$$

in which lu is the length of unbraced segment of a beam,

E is the modulus of elasticity of steel,

Iy is the out- of- plane moment of inertia,

G is the shear modulus

J is the torsional constant,

and *Cw* is the warping constant.

The critical moment solution *Mu* is derived assuming that both ends are simply supported relative : *u* and angle of twist θ , i.e. *u*= *u* ' = θ = θ'= 0 at both ends.

The standards then apply various modification factors to the expression to adapt it to other forms of loading and boundary conditions. any cross-section acts as a rigid disk within its own plane,

1) shear strains within the middle surface of the beam are considered negligible.

The first Vlasov assumption neglects the possibility of distortional effects within the beam. Consequently, it delivers a stiffer representation of the real beam and is thus expected to overestimate the elastic critical moments. Thus, the acceptance of the Vlasov theory-based equation in design standards involves the neglect of distortional effects. Towards this goal, Chapter 3 provides a study on the effect of various geometric parameters of a beam on it is ability to attain the critical moment as predicted by Eq. [2.1] for the case of uniform moments.

2.4 Standard Design Provisions

According to [21], the flexural carrying capacity of a laterally unsupported beam under bending about the strong axis is ruled by one of three possible modes of failure. These are:

1) elastic lateral- torsional buckling.

2) nonlinear- lateral torsional buckling, and

3) Plasticisation of the cross-section.

For the elastic lateral- torsional buckling mode, all standards use the classical lateral torsional buckling solution as an initial step to quantify the critical moment for a simply supported beam subject to uniform moments and account for non-uniform moment distributions by the introduction of standard dependent moment gradient factors EC3.

The first group of methods is used for beams subject to linear moment distributions.

The second category of methods is used for general moment distributions

Regarding the plastination of beams, all standards classify beam cross-sections into three categories:

1) Compact sections attain their plastic resistance prior undergoing buckling,

2) Non-compact sections exhibit local buckling after attaining their yield moment strength.

3) Slender sections to develop their yield moment capacity prior exhibiting local buckling.

2.5 Analysis of distortional dimensional effects

Generally speaking, any physical quantity can be expressed as a combination of force, length, or time

The Buckingham Pi theorem permits the reduction of the eight variables appearing in Eq. [2.1] into six independent dimensionless parameters. Therefore, the number of independent parameters is six dimensionless categories signified as product of the eight variables, each raised to an exponent as followsπi (i=1...6). A πi term is the product of the eight variables, each raised to an exponent as follows

$$[\pi i] = [Mcr]^{\alpha 1}[b]^{\alpha 2}[t]^{\alpha 3}[h]^{\alpha 4}[w]^{\alpha 5}[l]^{\alpha 6}[E]^{\alpha 7}[G]^{\alpha 8} \quad [2.2]$$

where exponents $\alpha 1$ through $\alpha 8$ must satisfy the following condition

$$(FL)^{\alpha 1}(L)^{\alpha 2}(L)^{\alpha 3}(L)^{\alpha 4}(L)^{\alpha 5}(L)^{\alpha 6}(E)^{\alpha 7}(G)^{\alpha 8} = F^0L^0 \quad [\ 2.3\ ]$$

For Eq. [2.3] to hold true, the following two identities must be satisfied

$$\alpha 1 + \alpha 7 + \alpha 8 = 0 \qquad [2.4]$$

$$\alpha 1 + \alpha 2 + \alpha 3 + \alpha 4 + \alpha 5 + \alpha 6 - 2\alpha 7 - 2\alpha 8 = 0 \qquad [2.5]$$

In a matrix form, the above two equations can be expressed as

$$[A]_{2*8}\{\alpha\}_{8*2=\{0\}_{2*1}} \qquad [2.6]$$

in which matrix $[A]$ is given by

$$[A] = \begin{bmatrix} 1 & 0 & 0 & 0 & 0 & 0 \\ 1 & 1 & 1 & 1 & 1 & 1 \end{bmatrix} \qquad [2.7]$$

$(\alpha)^T = (\alpha_1\ \alpha_2\ \alpha_3\ \alpha_4\ \alpha_5\ \alpha_6\ \alpha_7\ \alpha_8)$. Any solution for vector $\{\alpha\}i$ which meets Eq. [2.6], leads to an admissible πi term. The following is a possible set of six independent vectors

$\{\alpha\}i$ which satisfy Eq. [2.6]

$$[\{\alpha\}_1,\{\alpha\}_2,\{\alpha\}_3,\{\alpha\}_4,\{\alpha\}_5,\{\alpha\}_6] = \begin{bmatrix} \begin{Bmatrix}0\\0\\0\\-1\\1\\0\\0\\0\end{Bmatrix} & \begin{Bmatrix}0\\-1\\1\\0\\0\\0\\0\\0\end{Bmatrix} & \begin{Bmatrix}0\\1\\0\\-1\\0\\0\\0\\0\end{Bmatrix} & \begin{Bmatrix}0\\0\\0\\-1\\0\\1\\0\\0\end{Bmatrix} & \begin{Bmatrix}0\\0\\0\\0\\0\\0\\1\\-1\end{Bmatrix} & \begin{Bmatrix}1\\0\\0\\0\\0\\-3\\-1\\0\end{Bmatrix} \end{bmatrix} \quad [2.8]$$

Each vector$\{\alpha\}i$ corresponds to the terms π1=w/h, π2= t/b, π3= b/h, π4=l/h, π5= E/G, and $\pi_6 = M_{cr}/El^3$

The classical theory solution for the elastic critical moment M_u for a simply supported beam subject to a uniform moment is given by

$$\text{Mu}=\frac{\pi}{lu}\sqrt{EIyGJ + (\frac{\pi E}{LU})2IyCw} \quad [2.9]$$

When using th e3D modelling in FEA, the critical moment M_{cr} as predicted through an FEA buckling analysis, can capture the effect of distortional buckling. This contrasts with the elastic critical moment M_u which cannot capture and neglects such effects.

M_{cr}/M_u can be used as the sixth π term π_{6i} rather than $\pi_6 = M_{cr}/El^3$. With this substitution we have

$$f2(\frac{\text{Mcr}}{\text{Mu}},\frac{\text{w}}{\text{h}},\frac{\text{t}}{\text{b}},\frac{\text{l}}{\text{h}},\frac{\text{E}}{\text{G}}) = 0 \quad [2.10]$$

For steel, the dimensionless Parameter E/G is essentially constant, or

$$\left(\frac{\text{Mcr}}{\text{Mu}}\right) = f\left(\frac{\text{w}}{\text{h}},\frac{\text{t}}{\text{b}},\frac{\text{l}}{\text{h}}\right) \quad [2.11]$$

This means that the ratio of critical moment including distortional effects to the classical critical moment depends on only four dimensionless parameters that is w/h, t/b, b/h and l/h. Therefore, in the following sections, a systematic parametric study is conducted to investigate the effect of the above four parameters on M_{cr}/M_u

2.6 Literature review on the behaviour of cellular steel beams

Over the last decade, considerable research has been carried out on the buckling behaviour of cellular and castellated steel beams, focusing on different failure modes such as lateral-torsional buckling (LTB), lateral-distortional buckling (LDB), shear buckling and web-post instability (WPB). This section provides a brief overview of recent studies on these failure modes.

2.6.1 Lateral Torsional Buckling

One of the main issues addressed in the literature for the lateral torsional buckling phenomenon. Many published studies have focused on the effect of web openings on the

LTB resistance of WOB. For example, in [41], the resistance of cellular beams with uniformly spaced circular openings was investigated, with particular emphasis on the residual stresses induced during fabrication. The researchers proposed an improved design approach to improve the accuracy of the predictions.

Further analysis by [42] investigated the buckling behaviour of cellular beams with and without stiffeners, using finite element modelling in ANSYS. Their results showed that stiffeners significantly improved the stability and increased the critical load capacity. They also identified the main failure modes, including LTB, shear buckling, local web-post instability and weld failure.

In [44] the authors investigated the effect of web openings on the LTB resistance of WOB by means of both analytical and numerical methods. By applying the principle of minimum potential energy, they derived analytical solutions that were validated against ANSYS simulations, showing a strong agreement. In the same year, [44] used ABAQUS to evaluate the LTB resistance of cellular beams, taking into account post-fabrication residual stresses. Their study contributed to a proposed update of Eurocode 3 by introducing a new imperfection factor based on the magnitude of residual stresses, which was found to be accurate and conservative.

Further contributions came in 2024 as shown in [45]**.** who performed both experimental and numerical analyses on cellular beams with circular web openings. Their work led to new LTB design rules for Eurocode 3, particularly for spans between 7.5 m and 11 m. Also, in 2024[46], they analysed the elastic–plastic buckling of circular arched cellular beams. They concluded that structural stiffness increased with a higher rise-to-span ratio under mid-span loads, but declined above 0.35 for uniformly distributed loads. In 2024, another research study [47] in which a nonlinear reliability model for LTB using Galerkin's method and arc-length techniques was developed. Their work enhanced understanding of post-buckling behaviour and contributed to more accurate reliability assessments.

2.6.2 Lateral distortional buckling

In contrast to LTB, lateral distortional buckling (LDB) has been studied in detail due to its complexity and impact on structural performance. In 2018, Piassi et al [48]. focused on LDB in composite cellular beams, especially in regions subjected to negative bending moments. They developed a new equation for the calculation of rotational stiffness, which improved the prediction of the elastic critical moment for LDB. This formulation was validated by numerical analysis using ANSYS.

In 2020, the authors of [49] performed over 102,000 finite element simulations using Python to study LDB and overall buckling behaviour in cellular beams. Key influencing parameters identified included web opening diameter, web post width and flange thickness. In 2020 [50], authors investigated LDB in welded I-beams using GBTul and ABAQUS. They found that LDB significantly reduced resistance, particularly in beams with slender webs. While EC3 gave reasonable predictions, ANSI/AISC 360-16 and AS4100 required modification for greater conservatism.in 2021[51], authors analysed the effect of web distortion on LDB in castellated beams using nonlinear finite element models. Their results showed that LDB was most prevalent in medium slenderness beams with thin webs and that existing design codes (AS4100, EC3, AISC) tended to underestimate LDB capacity. Authors of [52] made a further contribution by evaluating the moment gradient factor (C_b) in I-plate beams, confirming its dependence on beam geometry and slenderness. Their results were consistent with previous studies on stainless steel I-beams and hollow tube flanges.

2.6.3 Web-post buckling and other failure modes

In addition to LTB and LDB, web-post buckling has been a major focus of recent studies because it can lead to local failure before overall buckling occurs. In 2022 [53], they conducted a study of WPB in cellular beams with closely spaced web openings. The study identified discrepancies in existing analytical methods for calculating WPB resistance, especially for narrow beams, and called for unified design algorithms. In 2023, another notable study by carried out extensive finite element analysis using over 15,000 ABAQUS models to investigate LTB in steel I-beams with sinusoidal web openings. The researchers proposed a novel analytical method to calculate the critical moment specifically for sinusoidal openings under different loading conditions. The accuracy of the model was confirmed by numerical results, providing valuable insights for design applications [54]. In the most recent study, in (2025) presented a detailed numerical study of the LTB behaviour of castellated steel beams with sinusoidal openings. They analysed seventy-two beams with variations in span length, flange and web slenderness and steel grade (250 MPa, 460 MPa and 690 MPa). The results showed that higher steel grades and optimised geometric proportions significantly improved buckling resistance. The study concluded that short-span beams exhibited better performance and provided practical insights into the structural design of castellated beams [55].

2.6.4 particular studies on cellular steel beams

Very recent work on examines the flexural performance of cellular stainless-steel beams (CSSBS) with circular web openings with experimental validation, statistical analysis, and sustainability evaluation. local yielding [56]. The study provides evidence to support the use of CSSBS in sustainable structural designs, and it demonstrates experimental values and models intended for practical use. The cyclic loading effect on the load–displacement capacities of beams with web openings designed to BS 5950 specifications is studied in [57]. As a result of the research, it has been determined that the mechanical properties of the beam subjected to cyclic loads and designed according to the golden ratio are closer to the perfect model.

Finally, research should continue to address modern design challenges, including incorporating the latest updates to international standards such as Eurocode 3. This direction will help to refine the understanding and prediction of buckling behaviour under different loading and geometric conditions.

CHAPTER 3:

BEHAVIEOUR OF A WEB-OPENING STEEL BEAM

3.1 General

In the study of a WOB, the following limit states are to be verified for any steel beam with web-opening must be considered either partly or totaly:

- Global overturning of the beam;
- Plastic behaviour of the flanges under normal force
- Buckling in the web plane of the compressed flange
- Shearing in the web;
- Shear distortion;
- Vierendeel mechanism;
- Deflection criteria.

3.2 Behaviour of a web-opening beam

3.2.1 Effect of opening on force distribution

According to experimental and analytical behaviour of stiffened BWO studies carried out in [58], the existence of an opening in the web of a profile leads to a disturbance in the flow of forces in the beam. Consequently, calculations must take into account to the singularity compared to a solid beam.

3.2.2 Failure mechanisms due to web openings

Owing for the presence of holes, global forces in the section can be transformed into local forces in both the top and bottom flanges. The global moment in the section is transformed into a couple of local normal forces, whereas the shear forces are distributed between the two flanges. Figure 3.1 shows the distribution transformation of global forces into local forces at the centre of the opening. Based on this of global forces distribution, various failure modes that may occur will be clarified in the following. The force distribution within the centre of the opening are clearly illustrated. In Figure 3.1.

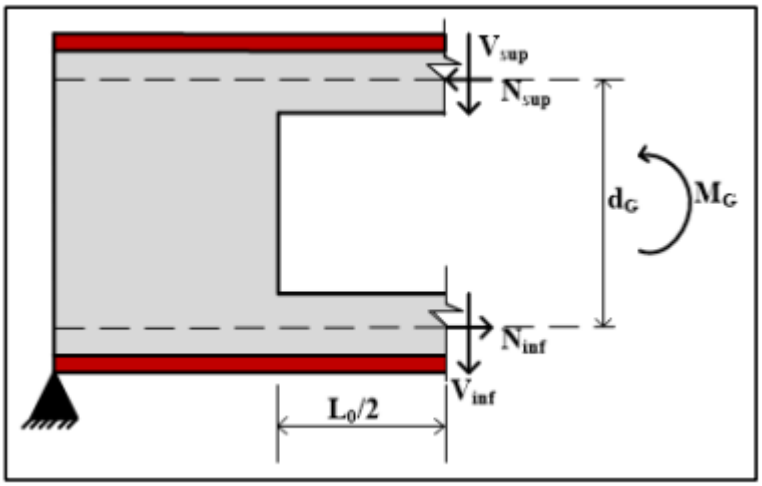


Figure 3.1 Force distribution at the centre of the opening

3.3 Openings Without Stiffeners

Early studies consider the impact and influence of openings on the behaviour of beams and how to find appropriate calculation methods. In subsequent sections some conclusions from various literature reviews regarding castellated beams are succinct details are given:

3.3.1 Early Studies on Castellated Beams

In [59], the author presented a method of calculation of the usual Vierendeel beam with "m" panels by reducing it to the solution of a system of "m" equations with "m" unknowns, each equation involved three unknowns except for the extremes, which have only two. Eventually, the solution to this system requires complicated calculations with many decimals. This solution is based on the calculation method as if the structure is statically indeterminate. More investigation with a direct, quick, and practical solution allowed reducing the calculation of a beam with only one unknown. the International Association of Beams and Structures published a study by Professor Stüssi in which the author proposes two principles for calculating statically indeterminate systems with a high number of unknowns [60].

3.3.2 Influence of opening shapes on structural performance

As stated by many researchers: Bower, Redwood and McCutcheon, Darwin Redwood and also Lawson [61]and Cho [62]; Oehlers and Bradford [63], the existence of web openings can meaningfully affect the load-bearing capacity of structural elements, depending on the shapes of the web openings. Many researchers have experimentally studied beams with various types of web openings. Usually the openings in the web are either hexagonal,

rectangular, circular, or oblong. Using FEM techniques, studies have shown that web openings with rhomboidal shapes lead to a reduction in stresses, which can be more concentrated at the sharp corners than in the circular shapes. Most previous studies considered the global analysis of a combination of forces acting on castellated beams. So, several parameters were included simultaneously, and different failure modes were attained, making it very difficult to determine which parameter affects the results in each specific case. At the present time, it is believed that different standards, as well as non-standard (irregular) web openings, need to be deeply studied considering isolated web openings (see Figure 3.2) [64]. Figure 3.2 illustrates Vierendeel bending considering two types of openings, that is hexagonal and rectangular perforations.

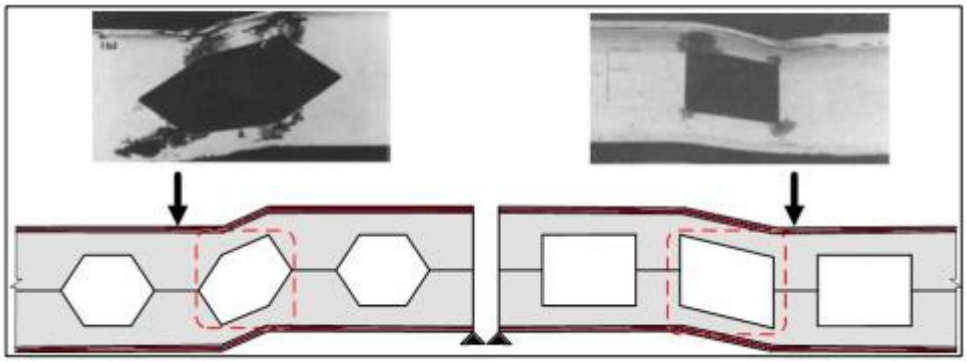


Figure 3.2 Vierendeel bending and formation of four plastic hinges [1].

Redwood [65] and later Chung et al. [66-67] wanted to characterise the resistance of openings based on the ratios of applied moment to resisting moment and applied shear force to resisting shear force for the considered shape opening. Equation 3.1 presents the interaction of the ratios and the global moment and shear forces applied at the opening. In the other hand, numerical studies have shown that the real resistance of the opening is often underestimated (by about 10 to 15% for the ranges of openings tested as demonstrated in [66], [68-69].

$$\left(\frac{Vsd}{V0,Rd}\right)^{2.5} + \left(\frac{Msd}{M0,Rd}\right)^{2.5} \leq 1 \qquad (3.1)$$

In fact, web openings lead to different stress distributions within the beam and introduce new failure modes. Experimental works on cellular beams often showed that exhibit three failure modes: 1) Firstly, the mode by buckling of the web's vertical member, 2) Secondly by distortion of the web between the end assembly and the first web opening, or 3) thirdly, a combination of both [70].

3.3.3 Numerical and experimental studies on beams with web opening

FEM modelling work Budi et al. [71] for the optimization of the size and distance of hexagonal openings in steel cellular beams is discussed and later verified through laboratory tests of steel cellular beam specimens. The obtained results showed that the resistance of steel cellular beams is increased by a factor of 1.938 to 2.041 compared to the original IWF. Better results were found for a beam with an angle of 60° and a width of opening between 0.186ho and 0.266ho with a good correlation between experimental and FEM outcomes. A numerical modelling study of a hexagonal-webbed beam under monotonic loading, Richard Frans et al [72]. The numerical modelling approach by means of Abaqus 6.11 is used to determine the opening angle and spacing between the hexagonal web openings within the beam and the von-Mises plastic failure criterion implanted in Abaqus was used to determine the failure load of the beam. There was no noteworthy difference between the numerical model and the experimental model (average difference of ± 10%). Experimental study on three steel beams and one composite beam was presented by Martin et al [73] along with 287 numerical simulations conducted in order to access the ultimate loads and failure modes under the combined effects of bending and shear. A new analytical calculation method was formerly proposed for the estimating the strength of cellular beams with a particular sinusoidal opening considering Vierendeel effect. A simplified analysis method of a steel cellular beam exposed to fire of restrained cellular steel beams (CSB) at high temperature, considering the inversion of deformation, Zhang and al [74]. This simplified analysis method is presented as an alternative to the finite element method. Besides, a finite element model was developed and validated by existing test results and numerical outcomes. The temperature distribution crossways the height of the section was assumed to be simply linear based on accessible research results. The simplified analysis method was then developed from equilibrium equations, constitutive equations, and geometric equations. A series of parametric studies using a verified numerical model were then carried out to evaluate the accuracy of the proposed method. It was found that the simplified method provided results that were in good agreement with those obtained from the finite element analysis (FEA).

3.4 Openings with Stiffeners

3.4.1 Influence of stiffeners on beam stability

To prevent local buckling effects, the need of reinforcing openings has captured the interest of researchers and engineers. Several solutions have been proposed thought out

experimental works and based on the theory of perforated beams. In the following a brief literature review is presented.

3.4.2 Types of stiffeners and their effectiveness

The reinforcement of the web near rectangular openings using horizontal plates is studied by Shrivastava et al. [65]. An experimental study was obligatory to determine premature buckling of beam sections typically considered in plastic analysis of structures. Main parameters that may affect the stability of the web near a stiffened opening are discussed as shown in Figure 3.3.

In Figure 3.3, it can be seen that the large deformations of the web and flange are rather misleading as they are mainly caused by a forced load on the beam after buckling became apparent. It is noticed that there was no significant sign of lateral movement (out-of-plane displacement), even at the maximum load, although no stiffeners were provided at the reaction points. The slenderness of the web was 1.79 for Beam UG1 and 1.7 for Beam VB-2 [65].

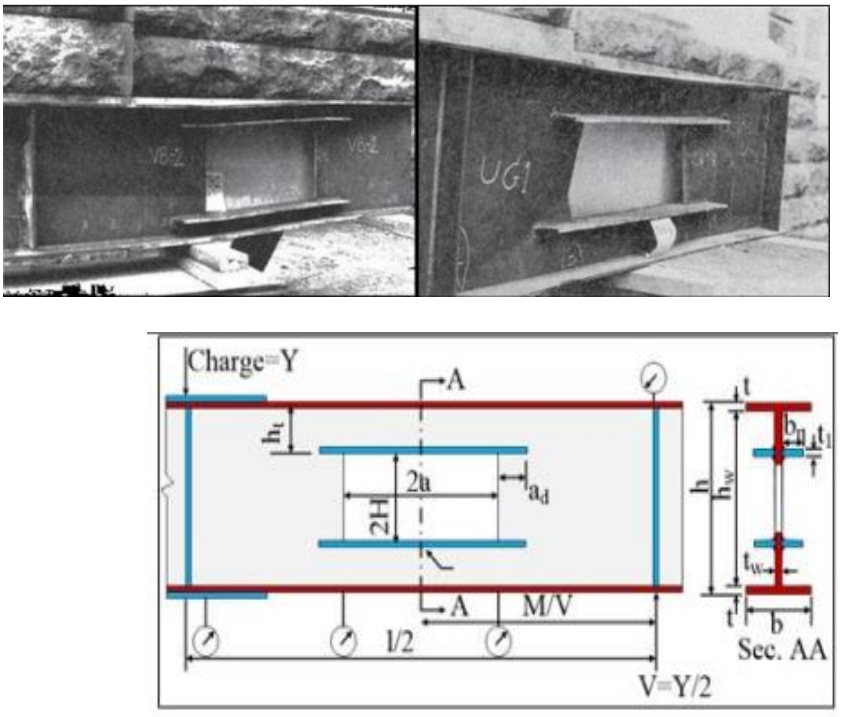


Figure 3.3 Terminology characteristics of tested beam and views of the UG1 and VB-1 specimens [2]

However, when plastic analysis is applied, certain slenderness limits are necessary. by using EC3 restrictions [12] or the annex N of the previous version of the Eurocodes, which a classification criterion for sections with rectangular openings is provided. It is suggested

that the stiffener contribution in resistance can be considered in terms of plastic resistance only with length of 20. The anchorage length of a stiffener is represented in Figure 3.4. If the stiffener does not meet this anchorage length, it cannot be considered in plastic resistance, but it can be taken into account in section classification. This then treats the web of the section as a T-section, not as a cantilever wall but as an interior wall [12][75][76].

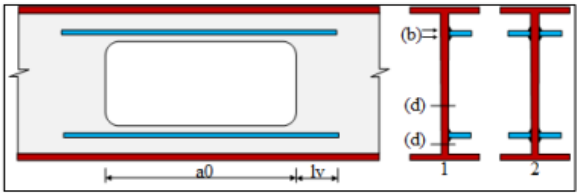


Figure 3.4 Stiffener anchorage length for horizontal stiffeners [3]

3.4.3 Experimental Studies on Stiffened Beams

An experimental study of nine full-scale perforated beams on perforated beams with elastic restraint beams where the test results are compared with results from other experimental, analytical, and numerical studies was presented by H. Showkati et al [77]. The objective was to access the performance and the effect of elastic reinforcements on the stability against overturning of these structural elements. Finally, experimental results and Finite Element Analysis (FEA) results are evaluated in light of the AISC 360-05 provisions. In the work presented in [78], results for ISMB 150 and 200 ISMB sections for perforated beams designed to attain a beam height 1.5 times the initial height. Further, the beam is analysed using FEM modelling (ANSYS14 software). Two load points are applied and it was observed that the stress concentration increases in the corners of the openings along the shear zone and at the load application point. Based on results from ANSYS14, the authors concluded that the shear resistance of the perforated beam can be enhanced by providing diagonal supports along the opening. The deflection of the beam, both with and without stiffeners, is studied.

3.4.4 Summary of the above literature review

As summary, it can be said that according to different literature sources, that failure of perforated beams occurs with the increase in the opening height and also due to the concentration of stresses around the openings. The effect of the opening height can be reduced by taking remedial actions by installing of stiffeners or by reducing the opening size through the usage of openings with variable heights. Also, stiffeners can be positioned

along the shear zone in such a way that stresses can be reduced, instability phenomenon can be controlled, and shear failure is minimalised.

3.5 Failure modes and structural analysis of castellated beams

3.5.1 General

In the particular case of a simply supported beam with a single span, failure occurs when the applied bending moment surpasses the bending resistance of the cross-section. Obviously, the resistance depends on the profile shape, the steel grade, and the classification of the section. Hence, its matter of verifying the section, with a possible interaction with shear forces, for example as shown in Figures 3 .5 to 3.7 below.

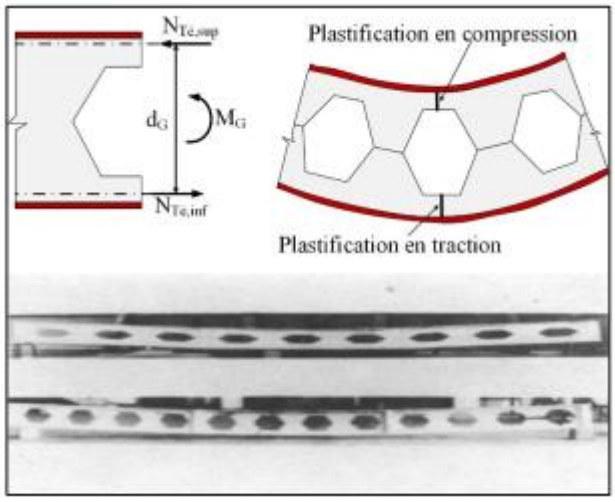


Figure 3.5 Bending failure of the beams with web-opening section [1].

Although current standards allow for openings with a height reaching 70% to 80% of the web height, the reduction in bending resistance is only 5% to 20%, due to the optimized distribution of material at the flanges of the section as stated in [18].

For the particular case of a long opening with a low flange height, the flanges may not reach their elastic limit and may experience local instability due to buckling in the plane of the web. EC3 requires that, for asymmetric sections with respect to the bending axis, the buckling resistance under bending must be verified considering the elastic properties, regardless of the section class. This verification can therefore be very restrictive in regions of high bending moments, it is not recommended to use openings that are both long (critical buckling length) and high (low moment of inertia of the compressed flange) as recommended in [19].

3.5.2 Vierendeel Bending

At the centre of the opening, the shear force is distributed between the two flanges. By writing down the equations of the equilibrium of the flanges, it appears that they are subjected to local bending due to the transfer of shear around the opening. This local moment is named the Vierendeel moment, in analogy with the mechanical behaviour of Vierendeel girders (ladder beams). As clearly shown in the figure bellow 3.6, the distribution of the local bending moment along flanges is linear and reaches two extreme opposite signs at the ends of the opening, the flanges, passing through zero at the centre of the opening, as shown in Figure 3.6 [63][79].

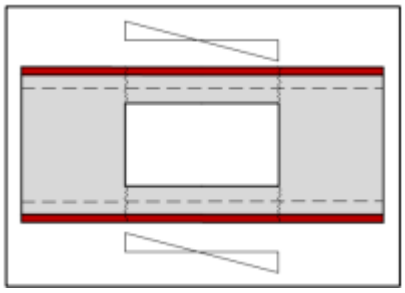


Figure 3.6 Moment distribution of local bending in the flanges

Then it is possible to reduce the local forces at the centre of the perforation to local forces at the corners of the hole, as shown in Figure 3.7.

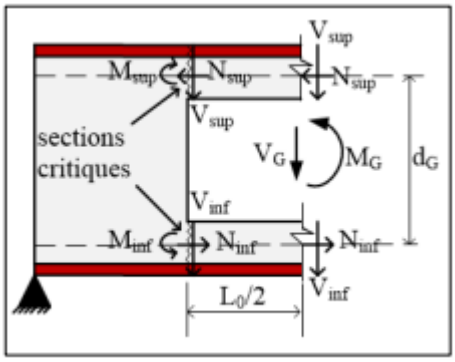


Figure 3.7 Local forces distribution at the corners of the opening

The local moments (or Vierendeel bending moments) in each of the four critical sections can be obtained by:

Moment Vierendeel=M_{sup} ($L_0/2$)

The normal force in a flange is expressed as:

$$N=\frac{MG}{dG}$$

With dG, the lever arm taken at an equal distance from the centres of gravity of the two flanges. Each corner of the opening is therefore subjected to a combination of normal force and bending moment (N, M) interaction.

The first plastic hinge will form at a certain level of loading. Any increase in load will causes a rise in internal forces values succeeding the new distribution until the second plastic hinge appears.

This continues until the four corners of the opening are fully plasticized, thus creating a Vierendeel mechanism (see Figure 3.8) [60].

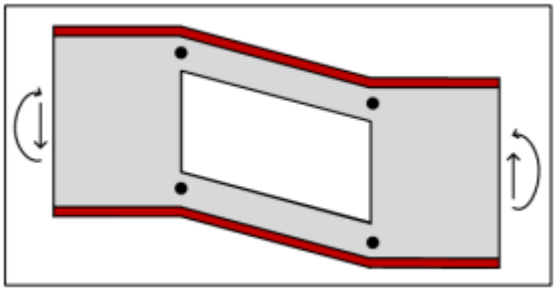


Figure 3.8 Plastic frame-type mechanism at the opening

The Vierendeel moment is compared to the resistant moment of the T-section at the corner of the opening, which corresponds to the plastic or elastic moment depending on the section's class. Then, the interaction between moment and axial force, as well as moment and shear force, must be considered. The second interaction involves calculating an effective thickness of the web. The moment-axial force interaction was initially considered linear in early models proposed in the literature [61]. Since this approach proved too conservative, the interaction is represented by a quadratic form for Class 1 or 2 sections and by a linear form for other classes [80].

The reduced plastic resistant moment due to the normal force is expressed as:

$$\boldsymbol{MN,pl,Rd}=\boldsymbol{Mpl,Rd}\times\left[\mathbf{1}-\left(\frac{\boldsymbol{N}}{\boldsymbol{Npl}}\right)\left(\frac{\boldsymbol{N}}{\boldsymbol{Npl}}\right)^{\mathbf{2}}\right]$$

The elastic resistant moment is expressed as:

$$\boldsymbol{MN,el,Rd}=\boldsymbol{Mel,Rd}\times\left[\mathbf{1}-\left(\frac{\boldsymbol{N}}{\boldsymbol{NPL}}\right)\right]$$

In the case of non-rectangular openings, Redwood suggests an adaptation of the presented methods by considering equivalent rectangular opening lengths. For example, for a circular opening, it is proposed to consider an equivalent rectangular opening with a

length (diameter of the circular opening) and a height (diameter of the circular opening) [65] and [80].

3.5.3 Shear in the perforated section

The shear resistance of a section is proportional to the shear zone as shown in Figure 3.9-a), which is in turn is mainly formed by the area of the web. Therefore, the presence of an opening directly reduces the shear area, and consequently, the shear force that can be resisted by the section, Figure 3.9b is being weakened. As a result, the presence of an opening with a height representing 75% of the web is likely to reduce the shear resistance of the perforated section by a similar proportion.

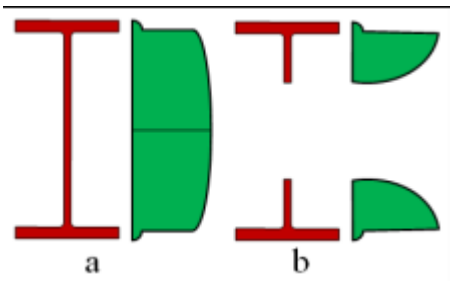


Figure 3.9 Shear stress distribution (a) a solid web section (b) T-members

The determining the distribution of shear force between the flanges is very important issue when analysing an open-section beam. A general practice is to consider a distribution proportional to the shear area. Still, this is a simplified approach that deviates from real situation as the asymmetry of the section increases reported in[20].

3.5.4 Shear Buckling of the Web Panel

It is well known that the presence of compression in an element indicates that there is a potential possibility of instability. In the case of a steel section, the web panel undergoes indirect compressive forces related to the shear of the beam as shown in Figure 3.10. Therefore, it is necessary to check out the condition of stability of the web panel against shear buckling [81].

According to reference [82], the buckling behaviour of a compressed plate can be compared to the buckling of a column. When the critical buckling stress is reached, the panel buckles due to compressed diagonal. The fibres perpendicular to the direction of compressive stresses develop tensile membrane forces (see Figure 3.11). This tensioned diagonal faces the panel's deformation, thus increasing the load-carrying capacity until this diagonal fails.

In this post-critical domain, the compressed diagonal can no longer support more forces, and the beam then behaves like a PRATT truss.

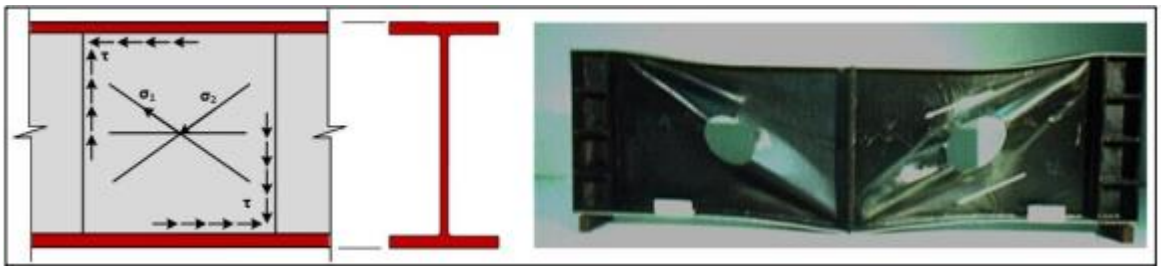


Figure 3.10 Principal compressive and tensile stresses in a panel and a beam with web openings under shear [19]

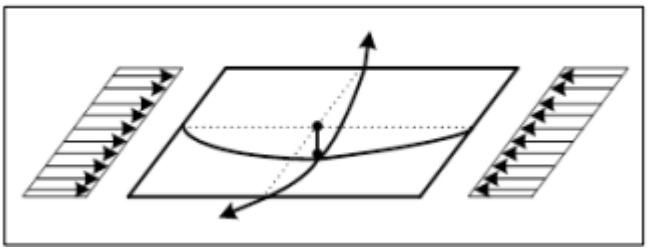


Figure 3.11 Membrane action stresses in a plate under pure compression

Evidently, the presence of an opening reduces the dimensions of the panel's diagonals, thus, reducing the forces that can pass through them (see Figure 3.12). This increases the vulnerability of the web panel to shear buckling.

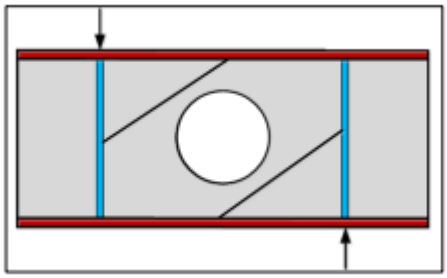


Figure 3.12 Tensile diagonal field in a perforated panel

An analytical model was developed to verify the shear buckling resistance of a slender web panel with an isolated opening. This shear buckling resistance is given by:

$$\boldsymbol{Vbw,Rd}=\mathbf{0.9}\boldsymbol{Vb,Rd}\left(\mathbf{1}-\frac{\sqrt{\boldsymbol{d0L0}}}{\boldsymbol{hw}}\right) \qquad \text{Equation 3.1}$$

Where V_{bw} the shear buckling resistance according to EC3-1-5 §5.2 [EC3-1-5] [84]. In addition, for a circular opening with, this method follows the formulas of Eurocode 3-1-5,

which are based on models considering the effect of a tension field. Consequently, this method is only applicable to isolated openings [83]

3.5.5 Buckling of the Web Post

When two isolated openings are close to each other, the web post located between these two openings is exposed to longitudinal shear that must be checked [17].

For the case of a castellated beam, the intermediate web post is also disposed to buckling in the form of double curvature out of the web plane, as illustrated in Figure 3.13. The maximum curvature is observed at approximately $\pm 0.45h0$ from the mid-height of the post. The position of the critical section is influenced by the condition of symmetry or asymmetry of the cross section, the size of the web post, and the load conditions. It should be noted that the deformation is not exactly symmetrical for the two curvatures, as the tension flange opposes instability, which reduces the deformation.

An analytical calculation model is proposed in references [84][85].



Figure 3.13 Buckling of the intermediate web post of a castellated beam [44]

3.5.6 Lateral -torsional buckling

Alike solid beams, the most predominant failure mode for a castellated beam is lateral-torsional buckling. This mode is occurring when a change in the plane of loading and a rotation of the section about the longitudinal axis of the beam, as clearly illustrated in Figure 3.14.

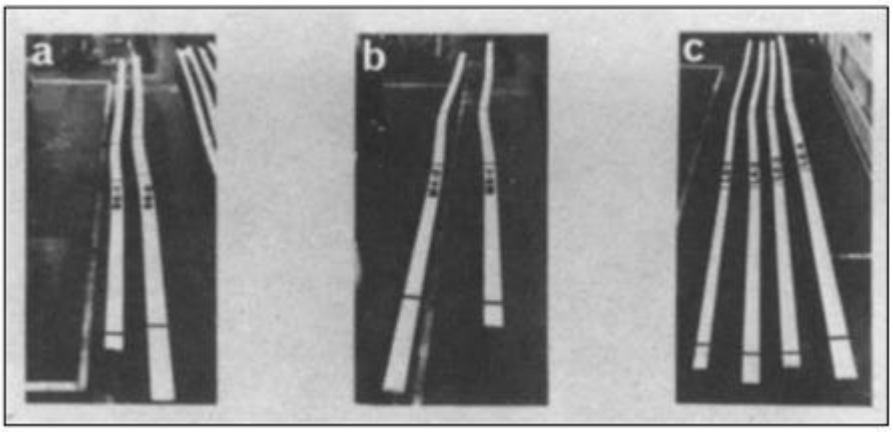


Figure 3.14 Beam tipping [1]

The torsional - flexural rigidity, relative to the weak inertia axis, opposes the lateral-torsional buckling, the main component of torsion is due to the presence of the web openings, which enable the deformation.

3.5.7 Additional Deflection

Web openings reduces the shear and flexural rigidity of the beam which leads to a greater deflection compared to a solid web beam of the same size. According to [66], for the case of hexagonal openings, the additional deflection can reach up to 2% compared to a solid web beam which becomes up to 20% for circular openings,

The stress concentration can be observed in the mechanical design of components or mechanical parts. This phenomenon is characterised by a local increase in stress in a specific area, resulting in geometrical changes. The areas with high stress concentration are often caused by fatigue, which can lead to crack propagation and, in severe cases, catastrophic failure in brittle materials, Figure 3.14 [86].

For a given type of loading, the actual stress (if it is below the plastic limit) and the nominal stress at a point depend on the applied load. The choice of a coefficient representing the stress is inherently based on this context. The index “t” is used to determine the theoretical parameters and calculations that comply with the assumptions of elasticity theory. The mathematical expression, introduced by Peterson in his later works [89], applies to simple geometric forms in tension. The proposed equation for calculating the coefficient K_t is:

$$K_t=1+2\sqrt{\boldsymbol{a/\rho}}$$

where is the notch angle and is the radius of curvature.

In the case of a hole, a = ρ hence $K_t = 3$

K_t where, the maximum stress concentration in a discontinuous area (such as at a notch or hole) can be related to the stress in the net section:

$$\boldsymbol{Kt = \sigma reelle / \sigma nom}$$

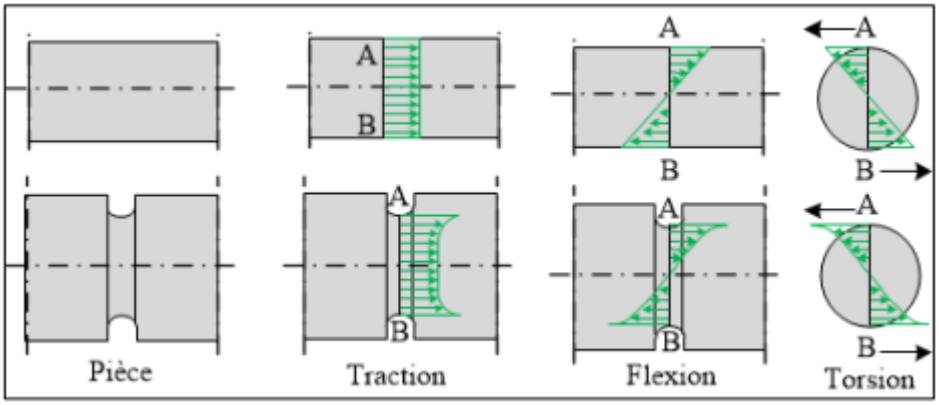


Figure 3.15 Stress distribution in different parts of a component under various loading conditions: tension, bending, and torsion.

Also, the stress concentration can be calculated by means of numerical methods, such as finite element analysis, or through analytical methods for simple geometries. Experimental methods, such as photo-elasticity, strain gauge methods, or thermal techniques, are also useful in determining stress concentration. In [87] a discussion the disadvantages of castellated beams. It is noted that the structural behaviour of castellated beams differs from that of solid beams. The load-carrying capacity of the web is limited, and the web does not provide sufficient support for short spans carrying heavy loads. The configuration of openings in these beams significantly affects their performance. The placement and size of these openings cause varying stress concentrations and limit the use of castellated beams in high-dynamic load conditions.

CHAPTER 4:

NUMERICAL LINEAR EIGEN FINITE ELEMENT ANALYSIS FOR LTB: CASES STUDIED

4.1 Finite element method and its concepts

4.1.1 General

The Finite Element Method (FEM) is one of the most noteworthy advancements in computational analysis in structural engineering. Originally developed for analysing weight-critical aerospace structures.

Unlike framed structures, where exact solutions to differential equations can exist, continuum structures require numerical approaches which are based on energy principles, that is the virtual work theorem and the principle of minimum potential energy criteria. Back to 1956, the advance of FEA traces Turner et al, who introduced it as a computational method for solving complex engineering problems. By the late 1960s, FEM was reformulated using weighted residuals and variational calculus, extending its applications beyond structural mechanics to include fluid dynamics, thermo-mechanics, and electromagnetics. Many influential books have formed its modern applications: Bathe and Wilson (1976), Zienkiewicz (1977), Cook (1981), and Bathe (1996). More recently, it has been applied to multi-physics problems, such as studying the effects of temperature on electromagnetic properties that influence electric motor performance [Khanani 2013].

4.1.2 Steps in Finite Element Analysis

The FEA process consists of some key steps which are:

1. Defining the geometric model that is representing the structure and discretizing it into finite elements.

2. Selecting element types that is choosing between bar, beam, shell, or solid elements which depends on the kind of structure, analysis type, and the required accuracy.

3. Assigning material properties involving the mechanical properties of the material with defining elasticity, yield limits, and nonlinear behaviours if applicable.

4. Applying loads and boundary conditions includes the external forces definition, moments, and constraints to simulate real conditions.

5. Generating the stiffness matrix by establishing equilibrium relationships between forces and displacements using stress-strain rules.

6. Solving the system of equations through the unknown displacements determination for computing stresses and internal forces.

The governing equation for finite element analysis is typically represented as: $Ku = F$.

In this work, FEA is used to provide valuable insights into the buckling behaviour of steel structures beyond code specifications. It also allows a better understanding of empirical equations

in cases where nonlinear material and geometric effects are significant and often neglected in standard design codes [89].

4.2 Buckling of members

4.2.1 General

Buckling is a structural phenomenon that happens when a component under some forces deforms suddenly in a lateral direction. This phenomenon does not unavoidably fails in material planification or even in a fracture, but it is taken as a failure mode because, subsequently, the member loses its ability to support supplementary loads. In fact, this lateral deformation meaningfully affects by reducing the member's stiffness and load-carrying capacity.

Studying buckling phenomenon is vital act in structural engineering because it directly impacts the safety and performance of structures. An accurate prediction of when and how buckling occurs allows the design of more reliable systems.

Generally speaking, a study of the stability of structures aims at calculating the elastic critical load and deducing appropriate design loads for elements under compression and /or shear to ensure that buckling does not occur. This is normally a complex procedure although the techniques can be built up from the matrix analysis methods are available. Luckily, the stability analysis of a structure can be considered subsequent to the linear elastic analysis. Further, in many cases Codes of Practice by sufficient guidance, specify where a stability analysis is not to be necessary. Nevertheless, important kind of structures are prone to stability analysis and, fortunately, the computational effort required is continually being reduced by developments in computer applications.

4.2.2 Lateral torsional buckling of bending members

Owing to twisting around its longitudinal axis, a bent member can fail by Torsional buckling phenomenon. This type of failure mode is frequent in the case of members under compressive loads where the whole section rotates or twists as an entire rigid body. This phenomenon occurs under pure compression where a significant component of torsional stress exists.

LTB is considered as a critical situation for laterally unsupported beams. Like members in compression, the resistance of members in bending to lateral torsional buckling depending on several parameters: the non-dimensional slenderness and mainly for post-buckling analysis an allowance for initial imperfections. But no simple equation exists for non-dimensional slenderness for LTB. The value of Mcr is to be derived from the elastic critical buckling moment. In EC3 for instance, there are two methods for determining LTB slenderness manually without the need to determine elastic

critical moment. Both are based on empirical simplifications and giving conservative values of slenderness.

4.3 Solution by Finite Element Analysis for buckling problems

4.3.1 Introduction

Software tools like Abaqus, Ansys etc. are precious tools for performing buckling analysis, enabling precise modelling of this complex behaviour. The using of finite element analysis software (LTBEAM; ABAQUS ; ANSYS) is becoming an issue for instability problems when using matrix analysis when is not possible to isolate uniform structural components under a complex loading or when the interaction between members makes it difficult situation where determining boundary conditions for the critical member.

Two types of buckling analyses i.e. elastic buckling analysis and non-linear post-buckling analysis can be performed to estimate the ultimate load carrying capacity of beams. Firstly, an eigenvalue analysis is performed for elastic buckling analysis in which eigenvalues of corresponding Eigen modes are determined using the linear perturbation buckling analysis. For non-linear post-buckling analysis, finally, RIKS method implanted in ABAQUS is being selected since it is suitable for predicting the post-buckling as well as for understanding the non-linear behaviour of geometric collapse. RIKS method is based on Arc-length method and is a form of Newton-Raphson iteration method, in which an additional unknown, named load proportionality factor LPF is introduced to provide solutions for load and displacement. This will be entirely discussed in the following chapter5.

4.3.2 Performing Eigenvalue buckling analysis

It is assumed that the structure behaves linearly elastic manner n considering the linear stiffness of the elastic properties of the material. Also, the effects of initial imperfections are not introduced in first order analysis.

The first order buckling analysis is adequate for determining elastic critical buckling loads for most situations by ignoring the material non-linearity and geometric deformations.

The first result of an FE buckling analysis is a series of eigenvalues or the load factors (multipliers on the magnitude of the given loading) presenting the various buckling mode sat their critical state. When performing FE buckling analysis, the outcomes are presented in ascending order and only the smallest 1st mode are of interest. To determine the design resistance, the designer must study not only the eigenvalues but also the associated eigenvectors:

4.3.3 Assumptions and methods of analysis

The linear buckling accepts that the structure behaves linearly elastic up to the bifurcation point. This means that the material follows general Hooke's Law in elastic range. Consequently, the analysis only considers point where instability first occurs, point of bifurcation. Also, it does not account for post-buckling effects or imperfections.

In addition, a buckling mode shape represents the shape which a structure adopts at the point of instability. Mode shapes are relative but not absolute. In Abaqus, they are normalized so the main displacement component is 1.0. They show deformation patterns, not their magnitudes.

While an eigen-solver implanted in Abaqus is a numerical algorithm used to compute eigenvalues and eigenvectors. Abaqus offers two eigen-solvers:

- Subspace Iteration Method: very Efficient for models requiring fewer eigenvalues.
- Lanczos Method: which is Faster for large systems with many degrees of freedom.

4.3.4 Procedure of solving linear eigen buckling problem (ABAQUS)

The eigenvalue buckling analysis solves the following equation:

$$(K_0 + \lambda_i K_\Delta) v_i = 0$$

- Base stiffness (K_0): Initial Stiffness matrix of the structure
- Eigenvalue (λ_i): load multipliers which are solving for.
- Incremental Stiffness (K_Δ): which is the incremental stiffness matrix.
- Mode Shape or eigenvectors (v_i): the eigenvectors corresponding to the buckling mode shapes.
- Incremental load pattern defined in the Abaqus (Q):
- Abaqus operates and solve the linear buckling as follows:

1. **Set the Base State (K_0):**

- In case of a **preload** it performs a static analysis step first defying the initial stiffness matrix (K_0). .
- In case of no preload exists, it corresponds to the stiffness of the undeformed structure.

2. **Define the Incremental Load Pattern (Q):**

- In the "Buckle" step, describe the **pattern** of the live load Q.

3. Solve for Eigenvalues (λ_i):

Abaqus computes a series of eigenvalues **Interpretation of the Results:**

- Then Compute the critical buckling load using:

$$P_{critical} = P_{preload} + \lambda_1 Q$$

To Visualization module for results.

4.4 Introduction the used Software in this dissertation

In order to validate the model, set up in Abaqus, another open-source software has been used in this dissertation, that is LTBEAM devoted to Elastic Lateral torsional buckling developed by CTICM. Firstly, as it was the case with LTBEAM, an eigenvalue analysis is performed for elastic buckling analysis in which eigenvalues of corresponding Eigen modes are extracted using the linear perturbation buckling analysis.

The following two structural engineering software tools will be introduced:

- LTBEAM v1.0.11
- ABAQUS v6.14-1

The software described herein are referred to as LTBEAM and ABAQUS respectively. Information about their background will be given. Their methods for finding the elastic critical moment M_{cr} described and their possibilities and limitations in that area discussed.

4.4.1 LTBEAM

- **Introduction**

The "Centre Technique Industrial de la Construction Métallique (CTICM)" in France have established a computer program which enables the designer to rapidly calculate the elastic critical lateral torsional buckling moment in few seconds. The elastic critical lateral torsional buckling moment is determined by means of an iterative calculation procedure in which a linear eigenvalue analysis is realised. The behaviour of the beam is treated with a discretization which can vary from 100 elements up to 200 elements.

LTBeam uses FEM to obtain results. This software can be applied to straight beams with one or more spans under simple bending about their major axis. The cross section must be symmetric about the minor axis, but can vary along the x-axis. At the beam ends, the user can choose which one of them to restrain. The four DOFs are:

- Lateral displacement

- Torsion rotation

- Lateral flexural rotation

- Warping

Along the beam the following restraints can be applied:

- Lateral displacement, local and continuous

- Torsional rotation, local and continuous Supports conditions in the bending plane and externally applied loads are taken into account by the bending moment distribution.

- **User interface**

The program provides a database of different steel profiles.

The next step is to choose the support conditions at the end of the beam: allows the designer to apply one, two, or a continuous lateral restraint at different heights to the beam.

Many types of load combinations can be chosen.

The final step is to calculate the elastic critical lateral torsional buckling moment.

As a result, the value of the elastic critical lateral torsional buckling moment is given with a graphical deformed shape.

- **Simple input mode**

The user can also choose between 100, 120, 150 and 200 elements.

When lateral restraints are chosen with the alternatives fixed, and free or spring restraints are but for the end supports.

Different types of loading can be applied that is a concentrated point load, a distributed load and a point moment about the major axis.

The level of the forces can be chosen along the beam and the point load and the distributed load can be placed at different heights as well.

The cross section has to be constant along the x-axis in the simple input mode.

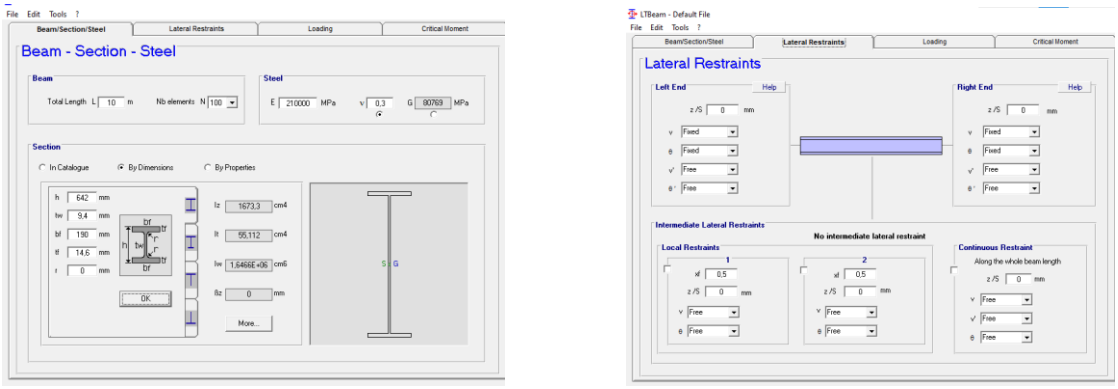


Figure 4.1 Introducing boundary conditions and load

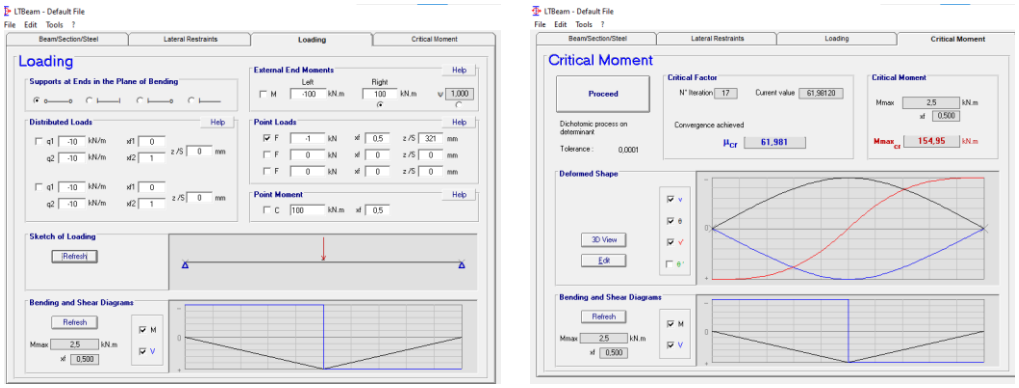
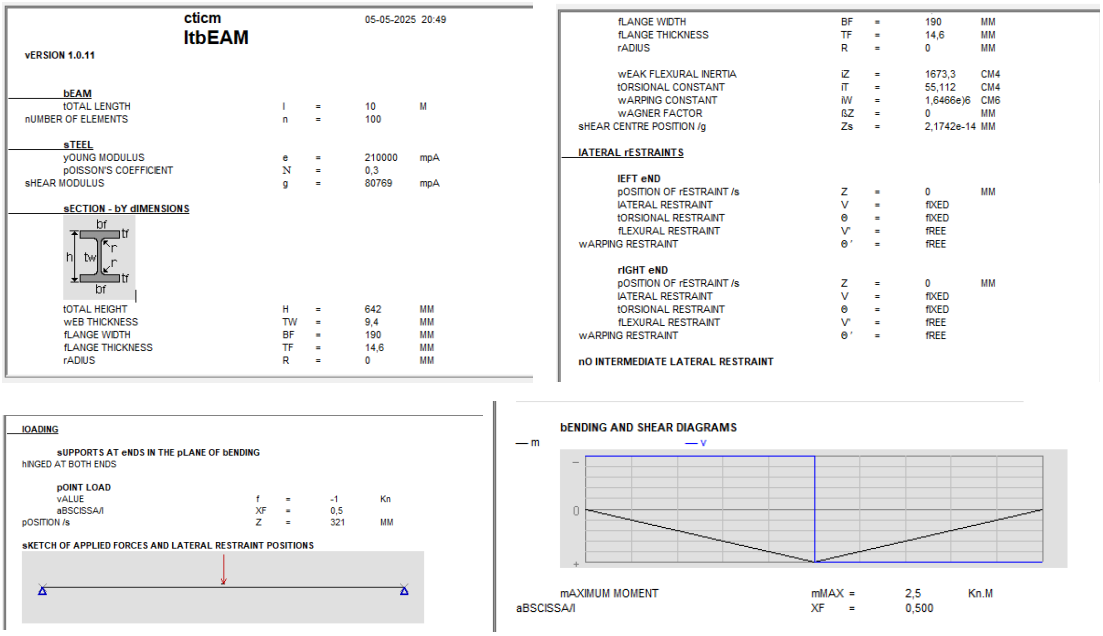


Figure 4.2 Introducing load position in the cross section



cticm
ltbBEAM
05-05-2025 20:49

vERSION 1.0.11

bEAM
tOTAL LENGTH L = 10 M
nUMBER OF ELEMENTS n = 100

sTEEL
yOUNG MODULUS e = 210000 mpA
pOISSON'S COEFFICIENT N = 0,3
sHEAR MODULUS g = 80769 mpA

sECTION - bY dIMENSIONS
tOTAL HEIGHT H = 642 MM
wEB THICKNESS TW = 9,4 MM
fLANGE WIDTH BF = 190 MM
fLANGE THICKNESS TF = 14,6 MM
rADIUS R = 0 MM

fLANGE WIDTH BF = 190 MM
fLANGE THICKNESS TF = 14,6 MM
rADIUS R = 0 MM

wEAK FLEXURAL INERTIA IZ = 1673,3 CM4
tORSIONAL CONSTANT IT = 55,112 CM4
wARPING CONSTANT IW = 1,6466e)6 CM6
wAGNER FACTOR ßZ = 0 MM
sHEAR CENTRE POSITION /g Zs = 2,1742e-14 MM

lATERAL rESTRAINTS

lEFT eND
pOSITION OF rESTRAINT /s Z = 0 MM
lATERAL RESTRAINT V = fIXED
tORSIONAL RESTRAINT θ = fIXED
fLEXURAL RESTRAINT V' = fREE
wARPING RESTRAINT θ ' = fREE

rIGHT eND
pOSITION OF rESTRAINT /s Z = 0 MM
lATERAL RESTRAINT V = fIXED
tORSIONAL RESTRAINT θ = fIXED
fLEXURAL RESTRAINT V' = fREE
wARPING RESTRAINT θ ' = fREE

nO INTERMEDIATE LATERAL RESTRAINT

lOADING

sUPPORTS AT eNDS IN THE pLANE OF bENDING
hINGED AT BOTH ENDS

pOINT LOAD
vALUE f = -1 Kn
aBSCISSA/l XF = 0,5
pOSITION /s Z = 321 MM

sKETCH OF APPLIED FORCES AND LATERAL RESTRAINT POSITIONS

bENDING AND SHEAR DIAGRAMS
— m
— V

mAXIMUM MOMENT mMAX = 2,5 Kn.M
aBSCISSA/l XF = 0,500

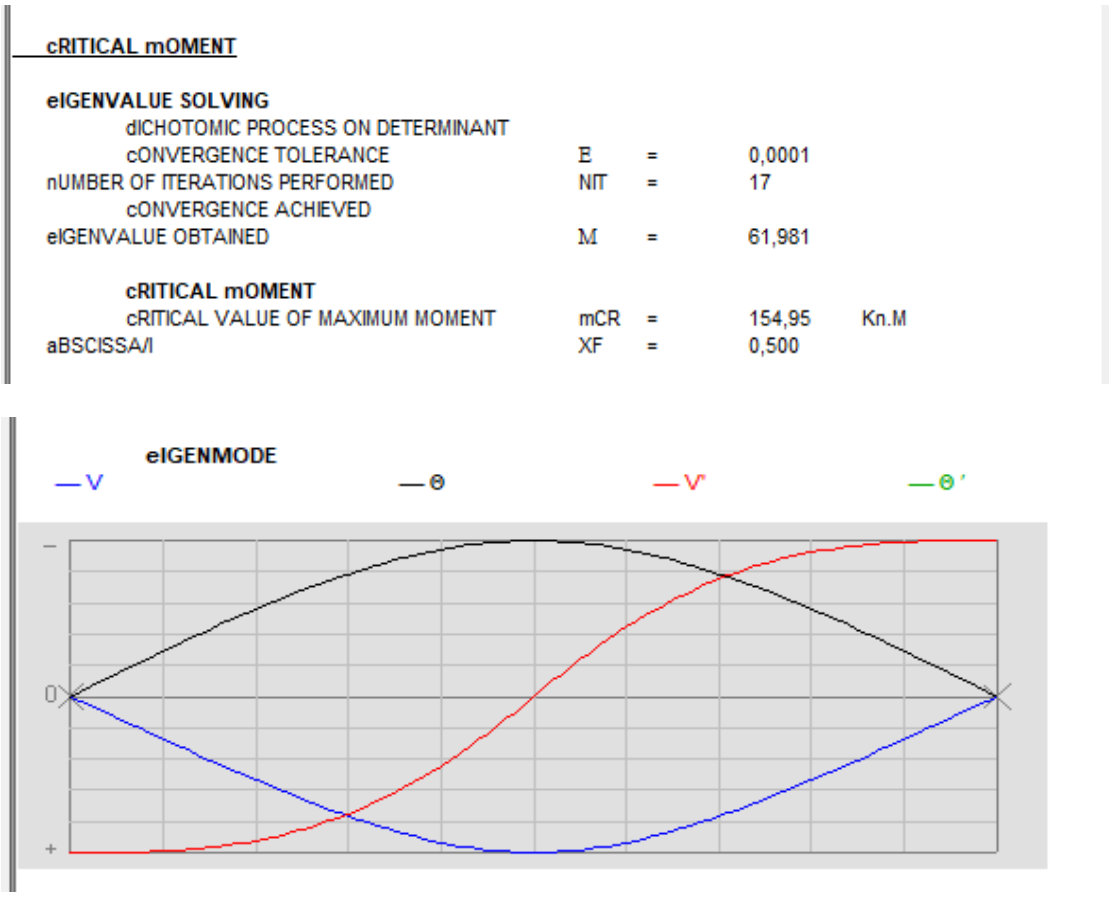


Figure 4.3 Calculation sheet from LTBEAM

4.4.2 ABAQUS Software for Elastic and Inelastic Buckling

- **Introduction** [90].

As well-known, ABAQUS is one of the leading software programs in the field of finite element analysis (FEA). It is used for simulating and analysing a wide range of engineering problems, as capable of handling nonlinear analysis, both in terms of mechanical behaviour and plastic materials, making it a powerful tool for structural analysis. Additionally, ABAQUS provides advanced contact modelling capabilities, considering large rotations and friction effects, which are essential for accurately simulating complex interactions between components.

Historically, the development of ABAQUS began in 1978 by Hibbitt, Karlsson & Sorensen, Inc. (HKS). The company was later renamed ABAQUS Inc., before being acquired by Dassault Systèmes in 2005.

Designed as a multi-purpose simulation tool, ABAQUS extends beyond stress and displacement analysis. It can be applied to various engineering fields, including heat transfer, mass diffusion, coupled thermal-electrical analysis, acoustics, soil mechanics (coupled pore fluid-stress analysis), and piezoelectric analysis.

Key Features of ABAQUS:

Capabilities for both static and dynamic analysis.

The ability to model large deformations of solids in both 2D and 3D.

A rich element library, including solid, beam, shell, and plate elements.

Advanced contact modelling for simulating complex interactions between solids.

A sophisticated material library, including elastic, elasto-plastic, concrete, soil, piezoelectric, and other material models.

The ability to analyse various engineering phenomena, such as vibrations, fluid-structure interactions, acoustics, and buckling problems.

ABAQUS/CAE (Complete ABAQUS Environment) provides an integrated and user-friendly platform for model creation, analysis, and visualization of simulation results. It is sub-divided into modules, where each module is devoted a specific aspect of the modelling process, such as defining geometry, specifying material properties, generating meshes, and setting up the analysis. The solver processes the generated input files, performs computations, and produces results that can be viewed and interpreted using ABAQUS/CAE [89].

With its extensive capabilities and user-friendly interface, ABAQUS remains one of the most powerful tools in finite element analysis, enabling engineers to conduct precise simulations of complex engineering problems with efficiency and trustworthiness.

- **Modelling sequence**

In ABAQUS, every complete finite-element analysis consists of three distinct stages:

Pre-processing or modelling: This phase is devoted to create an input file.

Processing or finite element analysis: This phase gives an output visual file.

Post-processing or generating the report, images, animations, etc. taken from the output file:

In fact, ABAQUS/CAE is skilled of pre-processing, post-processing, and monitoring the processing stage of the solver; but, the first stage can also be done by other compatible CAD software, or even a text editor.

In the following, some details will be provided for each module:

- Part Module: to define the geometry of the structural element or model to be analysed. Initially, a 2D geometry is formed and then manipulated to form a 3D geometry.
- Property Module: to define the material properties and cross-sectional elements that will be used in the analysis and assigns them to the appropriate parts.
- Assembly Module: to assemble the different parts together to form the global geometry of the model, even if there is only a single part.

- Step Module: to define the various types of analysis to be performed, such as linear or nonlinear analysis. It also allows you to specify which variables to include in the output files.
- Interaction Module: to define the interactions between different parts of the model, such as contact conditions or constraints using techniques like Tie or Rigid body.
- Load Module: defines the loads history and boundary conditions applied to the model at each step of the analysis.
- Mesh Module: by discretizing the model into finite elements, determining the type of elements and mesh density in order to ensure that the analysis is accurate.
- Job Module: describes the jobs that the analysis program will carry out, such as submitting the model for analysis after all the setup is complete.
- Visualization Module: used to view and post-process the results after the analysis, including stress distributions, displacements, reaction forces, and more. It offers visualization tools like surface plots, vectors, or contours.
- Sketch Module: used as a simple CAD tool to create additional drawings or make modifications to the parts before the analysis starts.

- Model Tree**:** which provides a graphical overview of the model and the objects that it contains, such as parts, materials, steps, loads, and output requests. Model Tree can be used to interchange between models.
- Results Tree**:** to offer a graphical overview of the output databases and other session-specific data such as *X*–*Y* plots.

N.B. There is no inherent set of units used in ABAQUS.

4.5 Linear Buckling Analysis (ABAQUS)

4.5.1 General

Performing (LBA) leads to determine the elastic critical lateral torsional buckling load of a beam., During this analysis, the bifurcation point is calculated by solving an eigenvalue problem. This eigenvalue problem can be solved when the stiffness matrix of the model becomes singular.

The software gives proposes two different methods to solve the eigenvalue problem, explicitly the Lanczos and the subspace iteration method. Both methods give the option for determining multiple eigenvalues.

The last stage is devoted to determine the elastic critical lateral torsional buckling load of the beam using the first mode of buckling., the applied load needs to be multiplied by the eigenvalue

resulting from the linear buckling analysis and subsequently, the elastic critical lateral torsional buckling moment can be determined using the first mode of buckling.

4.5.2 Steps to perform a linear buckling analysis (LBA)

- **Defining the geometry material and cross-sectional properties**

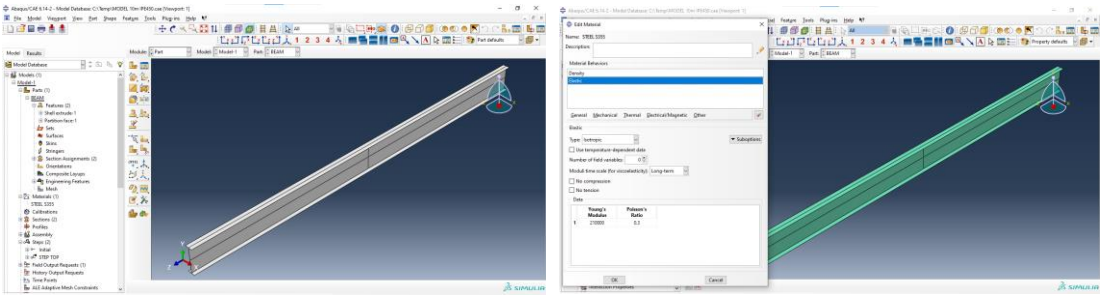


Figure 4.4 Typical model with material and geometric properties

- **Setting up the analysis**

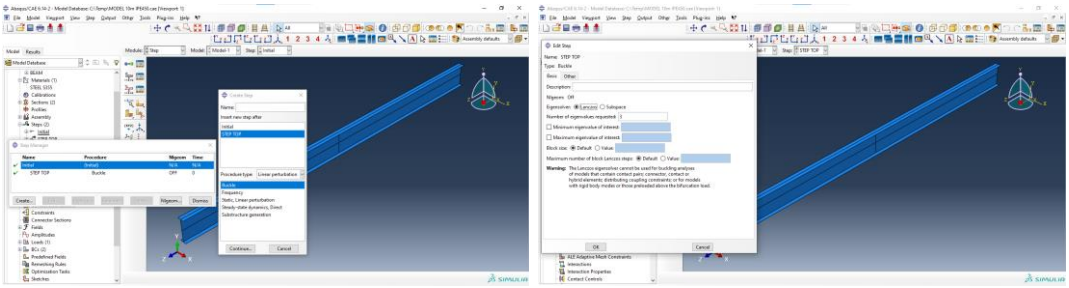


Figure 4.5 Setting-up the analysis

- **Defining the boundary conditions**

These conditions are defined in the Load module. The various boundary conditions are generated in a given Step and may be transferred to subsequent steps, see Figure 4.6

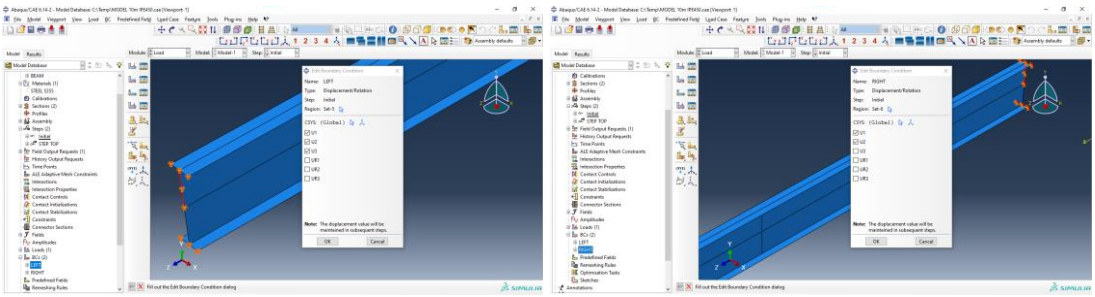


Figure 4.6 Defining the boundary conditions Boundary conditions

- **Defining loads**

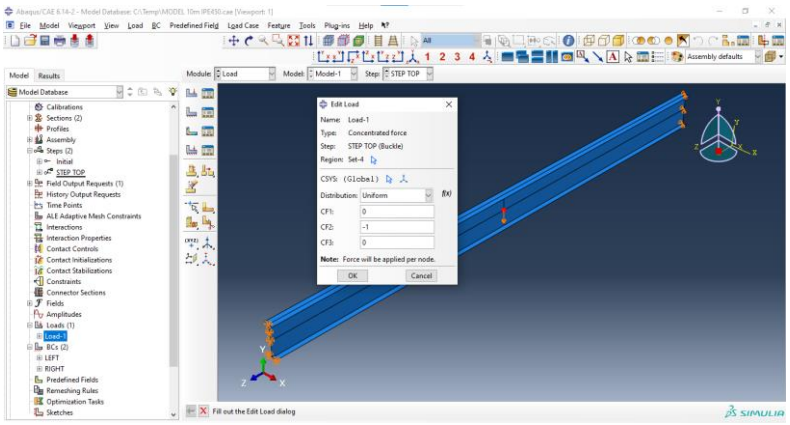
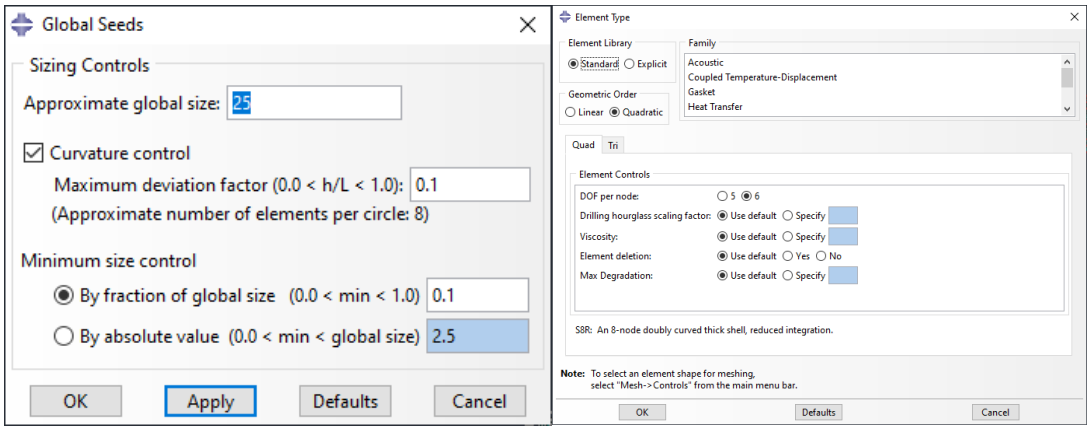


Figure 4.7 Defining the loads

- **Discretization**



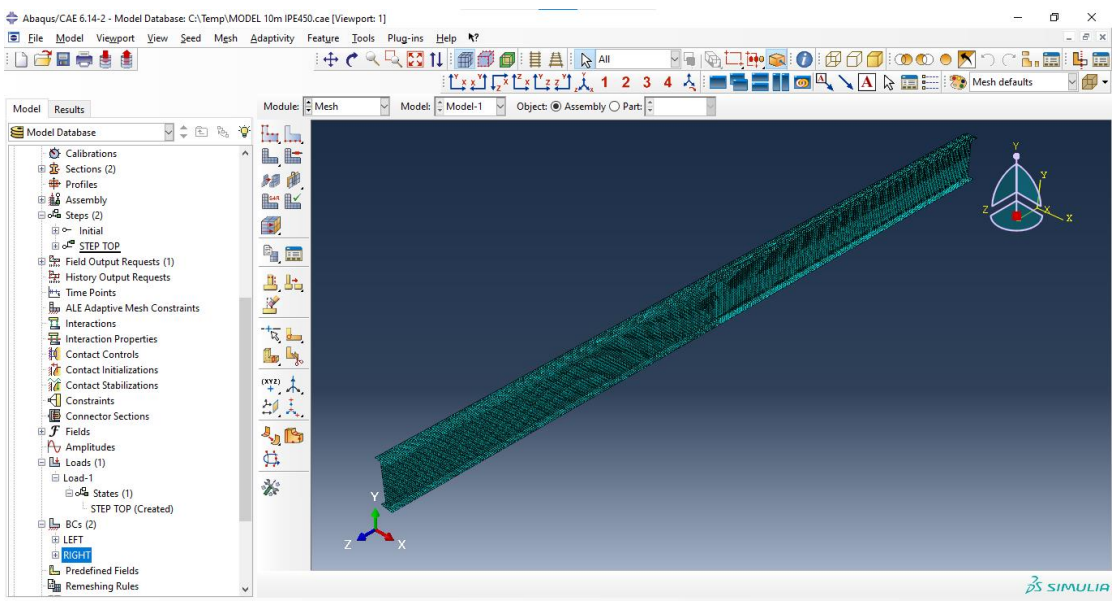


Figure 4.8 Discretization

Choosing the type of analysis

In the first step, only the elastic buckling analysis will be selected. This analysis will provide the Eigen values of different buckling modes.

Running the analysis

In order to submit the analyses to ABAQUS/Standard use the running module. This is the solver, which provides an output database that may later be accessed from ABAQUS/CAE.

Visualisation and post- processing of the results

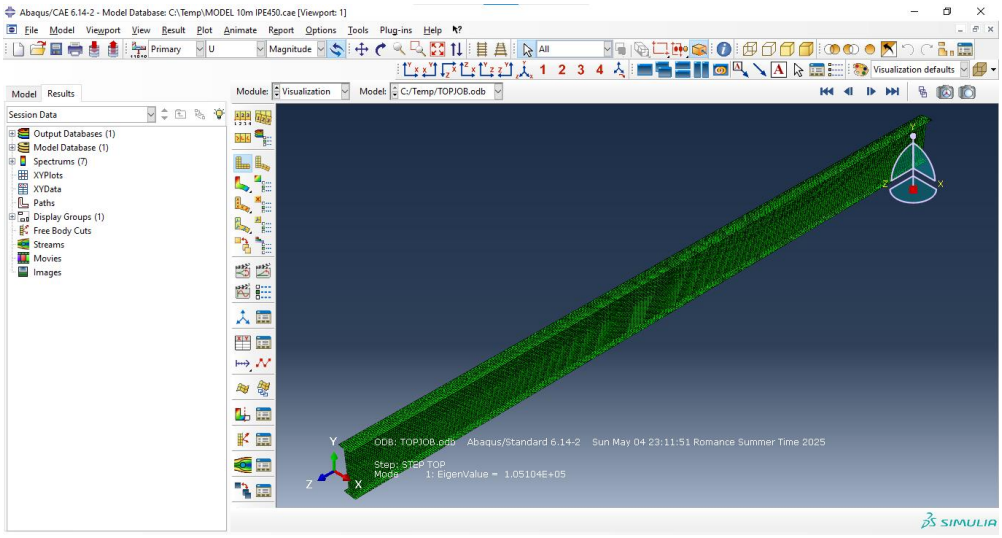


Figure 4.9 Visualisation and post- processing of the results

Result samples of Eigen analysis:

Mode 1

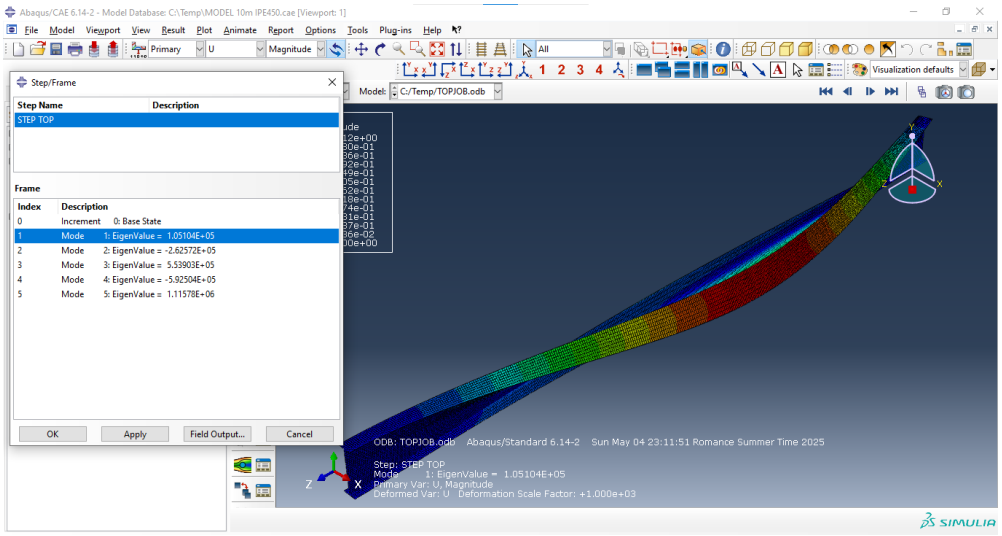


Figure 4.10 Linear buckling analysis deformed shape mode 1

Mode 2

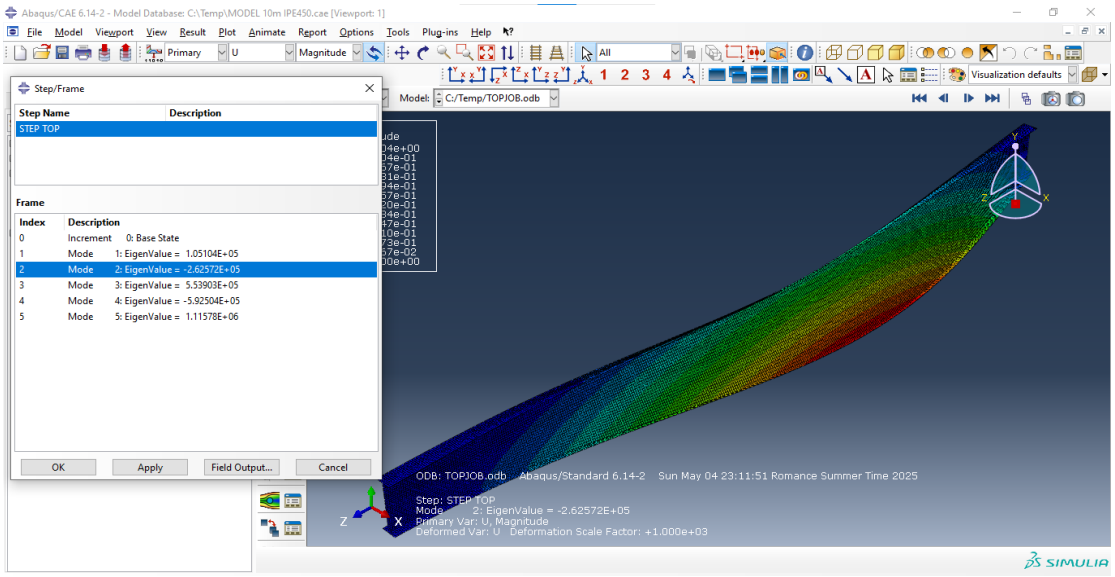


Figure 4.11 Linear buckling analysis deformed shape mode 2

4.6 Studied cases

4.6.1 General features of the numerical models

In this study, a numerical model was developed using Abaqus to analyse the structural behaviour of a BWO steel beam of section type IPE450. The total length of the beam is mm 10 m and it has been modelled using shell elements, which are suitable for the analysis of thin-walled members.

The section dimensions of the beam are based on standard specifications: IPE 450 with width = 190 mm; Flange thickness = 14.6 mm; Total height = 450 mm; Web thickness = 9.4 mm. Steel grade = S355, with linear elastic properties: Young's modulus E = 210,000 MPa, Poisson's ratio ν = 0.3.

Three different configurations were considered in terms of web perforation:

1. Reference beam without hole
2. Beam with a single web opening shape: circular; square and rectangular opening
3. Beam with several openings shape symmetry distributed along the web: circular; square and rectangular opening with central and no central opening.

A concentrated vertical load was applied at mid-span to simulate a common real-life loading condition, inducing bending stresses that could lead to buckling and provide insight into stiffness and stability behaviour.

- **Properties of modelled beams (see Tables 4.1 and 4.2 bellow)**

Table 4.1 Profile geometrical properties

Profile	**b (mm)**	**t_f (mm)**	**h_t (mm)**	**h_w (mm)**	**t_w (mm)**
IPE450	190	14.6	450	420.8	9.4
	I_y cm^4	I_z cm^4	I_t cm^4	I_w cm^6	W_{ply} cm^3
	33740	1676	66.87	7910000	1702

Table 4.2 Perforated profile geometrical properties

Profile	**b (mm)**	**t_f (mm)**	**h_t (mm)**	**h_w (mm)**	**t_w (mm)**
Perforated	190	14.6	450	642	9.4
	I_y cm^4	I_z cm^4	I_t cm^4	I_w cm^6	W_{ply} cm^3
	33740	1676	66.87	7910000	1702

- **Dimensioning the perforated beams L = 10 m and made of S355**

Three different geometric hole shapes were studied:

Circular opening: Diameter: do = 0.7h = 0.7 × 642 mm ≈ 449.4 mm

Square opening: Side length adjusted to approximately match the area of the circular opening. Sharp corners which likely cause stress concentrations.

Rectangular opening: Length and width defined by specific proportions such as lo ≤ 2do.

Fillet radius of r_o = 15 mm applied at corners to reduce local stress peaks

n the case of multiple openings, the spacing has been controlled to ensure that

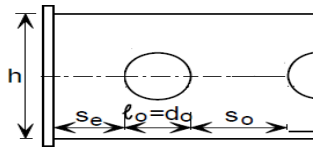
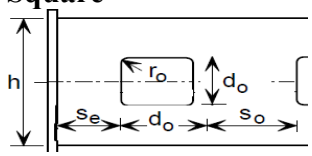
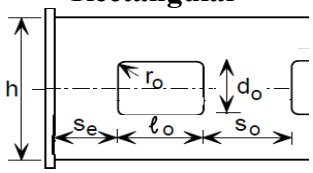
Se ≥ do for circular openings

Se ≥ lo for rectangular openings

Three different configurations were considered in terms of web perforation:

1. The reference solid beam without perforations
2. The beam with a single web opening: circular; square and rectangular opening
3. The beam with several openings symmetrically distributed along the web: circular; square and rectangular opening with central and no central opening.

Table 4.3 Geometrical details of web openings

Opening Shape	h (mm)	do (mm)	lo	Se condition	r_o (mm)
Circular 	642	0.7 × 642 = 449.4	—	Se ≥ do	—
Square 	642	≈ 449.4	—	Se ≥ do	15
Rectangular 	642	449.4	lo ≤ 2do (≈ 898.8 mm)	Se ≥ lo	15

4.7 Overall discussion

4.7.1 General

In this section, the results and the discussion of the linear elastic buckling for laterally unrestrained beams made from S355 are presented. The parameters investigated in this section are the effect of the localisation of the applied load and different web-openings configurations with and without holes in the linear buckling eigen elastic behaviour.

It is worth to recall that to analyse members in bending, shell elements were preferred for both the webs and the flanges. Generally, the FE mesh size should be sufficiently so fine that the model is capable capture and represent torsional effects in the elements and the overall buckling modes. The meshing must be fine to include to although not with accuracy unless the mesh is fine.

4.7.2 Validation of the model

As this dissertation is dealing with the linear and nonlinear behaviour of web-opening steel beams, a validation of models' set-up in Abaqus need to be validated. Another open-source software has been used in this dissertation, that is LTBEAM entirely devoted to Elastic Lateral torsional buckling developed by CTICM. Firstly, as it was the case with LTBEAM, an eigenvalue analysis is performed for elastic buckling analysis in which eigenvalues of corresponding Eigen modes are extracted using the linear perturbation buckling analysis.

Table 4.4 Validation of numerical models Abaqus vs. LTBeam model

Computed Critical Moment M_{cr} in kN.m			
Span Length L = 10 m			
Level of applied load	ABAQUS	LTBeam	Differences
Top flange	157.65	154.95	1 %
At centroid	247.53	224.96	10 %

Results are summarised in Table 4.4. Several temptations have been made to arrive at a model which matches with the LTBeam's one. Finding the adequate element type and meshing size, applying the right boundary conditions etc. As can be seen in Table 4.4, the differences in the prediction of Critical Buckling Moment, M_{cr}, varying from 1 to 10 %. See Figures 4.1-4.3 for LTBeam and 4.4-4.10.

4.7.3 Models with perforated web

Models with perforated web have been exclusively built-up in Abaqus. The first set of models are dealing with the case of single hole with different shapes operated at the left hand-hand side of the structure.

- **Single web-opening**

As it can be seen, the presence of opening in web section does influence the entire behaviour of the bending member according several parameters: to the number, the size and the location of this opening. The differences in % are computed regarded to the beam without any hole. In fact, one can see the difference showed in Tables 4.5 for the case of single web opening. It can be remarked that the circular and square openings give roughly same outcomes for a single opening and better results of M_{cr}, followed by the rectangular opening with the smallest values of M_{cr} being favourable. When the load is applied at the top flange, which is the most critical case, the differences vary from 1% to 6% for rectangular shape opening. For the case where the applied load is located at the centroid, the gap is bigger as it varies between 6 and 10 % in the same order as it was described for the first case. These differences show the decreasing of resistance against LTB compared to the same beam without any web opening.

Table 4.5 Effect of a single opening on LTB resistance of WEB

Computed Critical Moment M_{cr} in kN.m for a single opening by ABAQUS			
L = 10 m			
Case	Top flange	At centroid	Differences
No opening	157.65	247.53	
Circular	156.46	239.63	1% and 3%
Square	154.79	235.25	1% and 3%
Rectangular	148.38	223.84	6% and 10%

Some more details can be observed from Figures 4.12 to 4.14. Indeed, the elastic buckling e first mode of buckling which is the fundamental mode, of all studied case seem very likely same geometrical shape despite the shape of the opening made in the web with slight differences, the maximum value for rectangular hole. Same remarks can be made for the second mode of buckling with, of course, less interest.

Single circular opening

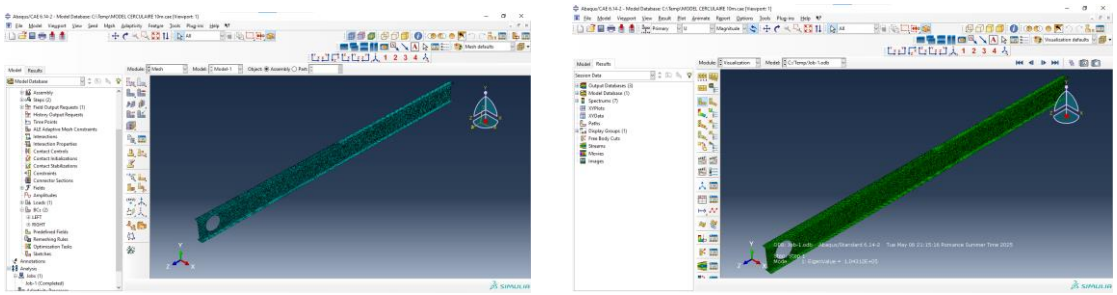


Figure 4.12 Discretization and Visualisation and post- processing of the results

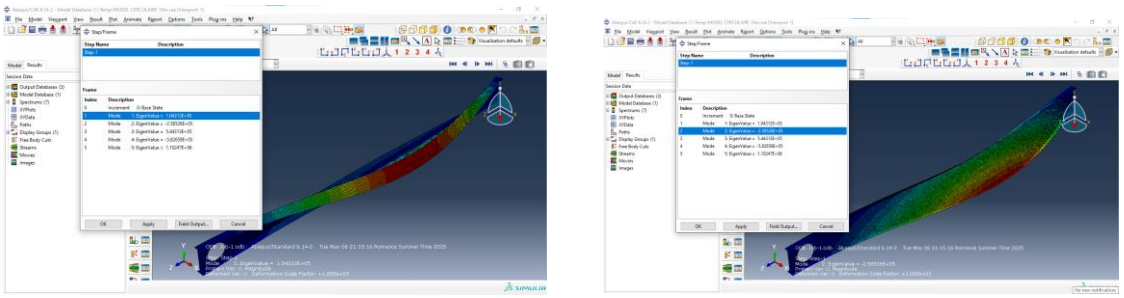


Figure 4.13 Linear buckling analysis deformed shape modes 1and 2

Single square and rectangular openings

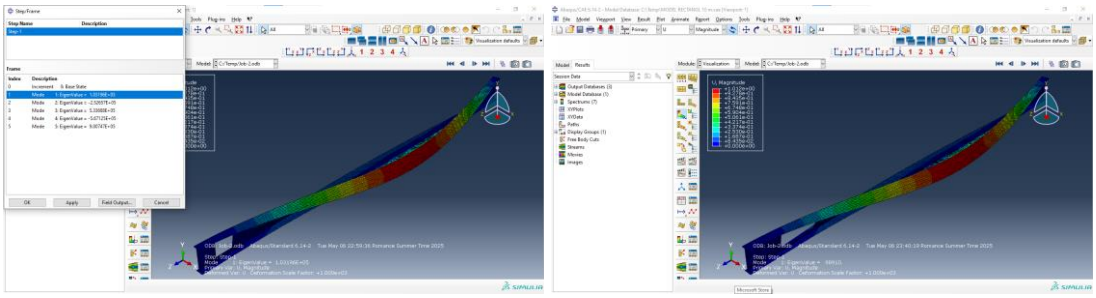


Figure 4.14 Linear buckling analysis deformed shape mode 1 for square and rectangular openings

- **Web with multi-openings**

It is worth to indicate that the number of cuts operated in the web is 10 for the circular and square perforations and only 6 for rectangular cuts. For the square apertures, a lateral distribution was adopted with five apertures on the left and five on the right, leaving the central region (load application zone) free of apertures. This configuration makes it possible to assess in what way the maintaining the stiffness in the midspan affects the buckling behaviour. In the case of rectangular openings, the configuration is a similar lateral distribution but with three openings on each side and no opening in the central zone.

For the case of multi-openings operated in the web section, once again, it has been found that the worst case is being the model containing rectangular hole shape even with a smaller number of opening (6 instead of 10 for circular and square openings). In fact, the difference follows to same.

Table 4.6 Effect of multi -openings on LTB resistance of web

Computed Critical Moment M_{cr} in kN.m for multi-opening by ABAQUS				
L = 10 m				
Shape	Number	Top flange	At centroid	Differences/ no opening
No opening	0	157.65	247.53	
Circular	10	139.74	225.67	12% and 9%
Square	10	134.66	217.85	17% and 13%
Rectangular	6	126.34	138.21	24% and 12%

- **Discussion**

As a primary conclusion of the LTB behaviour of the cases studied, the numerical results clearly show that the presence of web openings leads to a reduction in value of the critical lateral

torsional buckling moment (M_{cr}) compared to the reference solid beam without perforations. As previously discussed for a single circular opening, the reduction of strength against LTB phenomenon about 1% at the top flange and 3% at the centroid, indicating that such an opening has a limited influence on the global stability of the beam. However, when multiple openings are introduced, especially rectangular ones, a significant decrease in M_{cr} is observed, reaching up to 24% at the top flange and 12% at the centroid. This highlights the detrimental effect of recurring sharp-edged perforations on the buckling resistance of the beam. This behaviour can be attributed to increased stress concentrations around the corners and reduced web stiffness due to the Vierendeel effect.

When comparing the geometric shapes of the cuts, circular appear to be the most favourable in terms of minimising buckling effects due to the absence of sharp corners for other configurations. In contrast, square and rectangular openings create local weak zones that reduce the structural performance of the beam. Additional information is delivered in the following figures 4.15 to 4.16.

Circular (10 cuts)

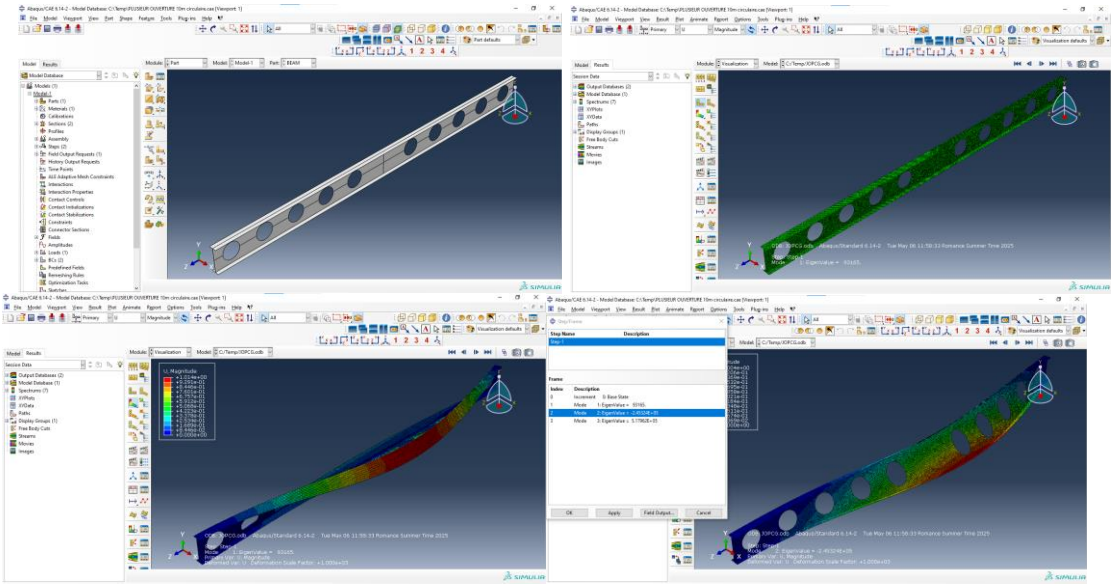
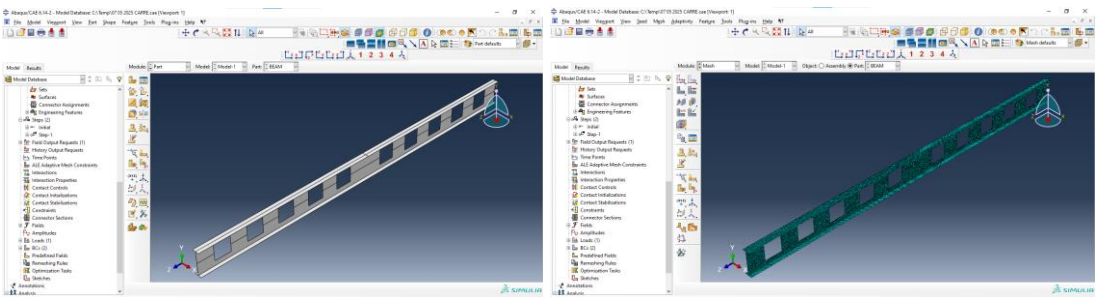


Figure 4.15 Discretization, Visualisation and mode shapes results

Square (10 cuts)



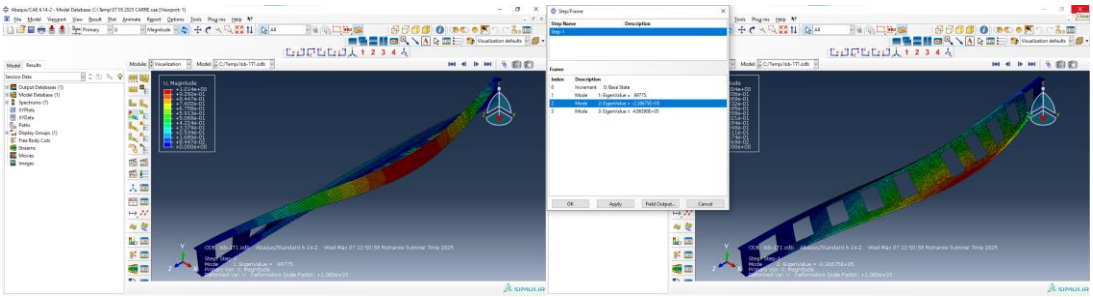
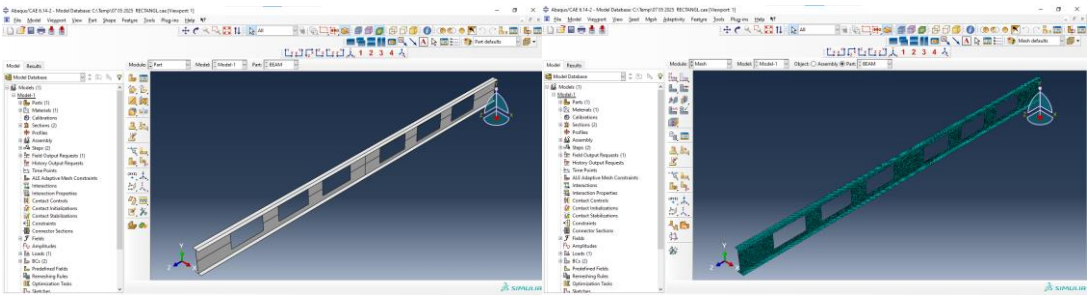


Figure 4.16 Discretization, Visualisation and mode shapes results

Rectangular (6 cuts)

Rectangular



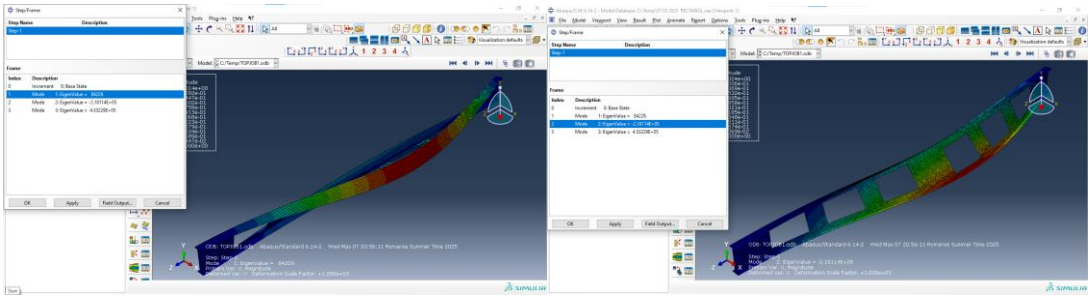


Figure 4.17 Discretization, Visualisation and mode shapes results

Additional models have been built-up in ABAQUS in order to better understand of how the number, the location and geometry of the web openings can affect the buckling resistance of the beam, especially in high stress regions, models with 11 holes being operated in the web for circular and square shapes shows slightly different values of M_{cr}. For rectangular second configuration which represents a more critical scenario where five consecutive rectangular openings were placed directly under the load application point with no spacing between them.

4.8 Conclusion

From the elastic linear buckling obtained results in this research work, it can be said that the strength of WOB to LTB is alternated by the presence of the different shape holes operated in the web section along with the level of application of the transverse load. The condition of applying the load in flange is the worst case with higher decreasing in the resistance for all configurations. The number, the geometrical shapes and the sizes of perforations is demonstrated to be determining parameters.

In addition, the symmetrical distribution of cuts along the web alters the buckling pattern. It can shift from a regular elastic mode to a more complex deformation shape depending on various parameters, with critical points moving to the most weakened regions. This explains the significant drop in M_{cr} observed in certain cases, particularly with multiple rectangular perforations, the weakest configurations. In fact, as the number of cuts increases, the reduction is not uniform for all shapes; openings with sharp corners - such as square and rectangular - tend to induce higher stress concentrations than circular openings. In addition, the symmetrical distribution of perforations along the web alters the buckling pattern. It can shift from a regular elastic mode to a more complex deformation shape, with critical points moving to the most weakened regions. This explains the significant drop in M_{cr} observed in certain cases, particularly with multiple rectangular perforations. It must be recalled that the work exposed in this chapter is the first step to a full numerical nonlinear lateral buckling behaviour of the perforated beam, which will be the subject of the subsequent chapter.

CHAPTER 5:

NONLINEAR NUMERICAL BUCKLING MODELLING OF WEB-OPENINGS SECTIONS: STUDIED CASES

This chapter deals with a numerical a parametric analysis carried out on unrestrained simply supported steel web opening steel structures in order to assess the elastic (eigen) and nonlinear buckling capacity using Abaqus software capabilities. An introduction to the nonlinear buckling post-buckling analysis background is given. The procedure of performing a full nonlinear post-buckling analysis taking into account geometric and material nonlinearity is carried out using ABAQUS is provided. The results of some studied cases will be presented.

5.1 Introduction to nonlinear buckling behaviour of structures

First of all, it must be recalled that the linear buckling analysis, discussed in the previous chapter, gives a rapid and conservative evaluation of the critical load by assuming perfect geometry and linear elastic behaviour. This consideration makes it acceptable for early-stage design process and safety checks. However, real structures are generally seldom perfect and frequently experience nonlinear behaviour before failure. So, to capture the accurate behaviour of a structure under loads, nonlinear buckling analysis necessary for a complete understanding. Geometric, imperfections, and material yielding, and post-buckling stability are taken into account for a nonlinear analysis

For the case of simple structures, eigenvalue buckling predictions (EBP) may be sufficient for design consideration; but if there is apprehension about material nonlinearity, geometric nonlinearity prior to buckling, or no stable post-buckling behaviour, a load-deflection, RIKS analysis implanted in ABAQUS must be performed to investigate the problem.

5.2 Nonlinear LTB post buckling analysis

In this section, firstly an introduction to the nonlinear buckling analysis the necessary background is given. The nonlinear analysis is essential when the buckling behaviour is influenced by the modified geometry of the structure

Failure studies of a structure’s post-buckling load-displacement using RIKS approach are often conducted in order to verify that the critical buckling load. They are also done to investigate the effect of more parameters such as an initial geometric imperfection on the load-displacement response of thin structures. An assumption must be made for the imperfection resulting from the combination of the eigenmodes associated and considering that the lowest eigen values is being the most critical.

The models are built-up in Abaqus to investigate the impact of lateral torsional buckling on the carrying capacity of web-opening steel structures is provide and discussed. The parameters investigated are: the number, the shapes and the sizes of holes, and the location of the applied transverse load. Initially, it was planned to carry out linear elastic and nonlinear buckling investigation on beams with different span lengths considering different steel grades. Unfortunately,

this task was not possible because of the difficulties risen-up when modelling the nonlinear post-buckling analyses and, of course, the luck of time.

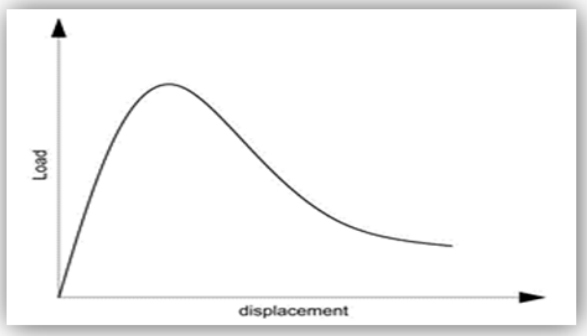


Figure 5.1 Probable non-linear buckling load-displacement behaviour

For a buckling instability of a member, the load-displacement shows a negative stiffness and consequently, the structure has to release strain energy to remain in equilibrium Figure 5.1.

5.3 Imperfection sensitivity of thin structures

As previously mentioned, geometrically nonlinear static problems sometimes include buckling or and a collapse behaviour.

The nonlinear behaviour of some structures depends strongly on the imperfections introduced in the original geometry, particularly if the different buckling modes interact. Then, to be assessed, the imperfection sensitivity of the structure based upon a single buckling mode tend to yield non-conservative results which can be done by changing the value of magnitude of the scaling factors of the several buckling modes. It is very common to perform many of analyses to study the sensitivity of a structure to imperfections.

N.B. 1. With a large value of imperfection makes the analyse easier. In this case, the development of the post-buckled behaviour will be smooth and fairly easy to analyse.

2. In the contrary, if the imperfection is small, the deformation will be quite small compared to the imperfection below the critical load. The response will grow quickly near the critical load, introducing a quick change in behaviour.

5.4 Over-all on nonlinear post-buckling using Abaqus.

As it was said earlier, the nonlinear buckling is needed to capture behaviour of structures in the actual scenarios and to capture events as the geometric imperfections, material yielding, and post-buckling stage.

Once a structure buckles really, its response habitually includes:

5.4.1 Unstable Behaviour of a thin structure

When performing astatic analysis, the load is the driving parameter. That is a specific load magnitude is applied and the solver calculates the resulting displacements. However, in nonlinear cases some differences must be mentioned, that is:

- The load-displacement relationship is not any longer linear.
- The structure may attain a bifurcation point of instability leading to large displacements or where the additional load.

- **Introducing imperfection Sensitivity**

Real structures are not perfect. Small imperfections in geometry leads to severely affect the when buckling occurs.

- **Introducing Post-buckling Behaviour**

Subsequently to buckling, the structure's response may stabilise that is it can carry more load or can simply destabilize by simply collapsing. Obviously, these kinds of behaviours cannot be captured by LBA. Then the RIKS method are required.

The modified RIKS method uses a tangent line of a function to intersect with an arc, situated at the end of every step. From this point on, the curve will converge over the arc-length until it reaches an intersection of the arc with the function. At this point, the step is completed and the process will continue with the next step (Figure 5.2).

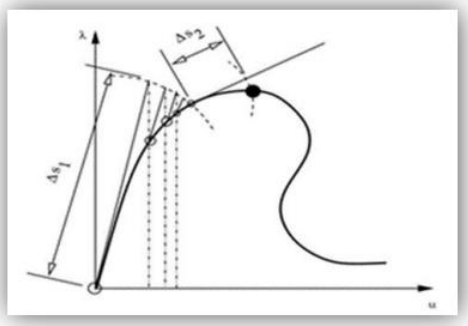


Figure 5.2 Example how RIKS method operates

5.4.2 Nonlinear buckling using RIKS method implanted in ABAQUS [90].

RIKS method assumes that all loads are scaled proportionally. It solves this by treating the load proportionality factor (λ) as an unknown variable. This means:

- Instead of straight specifying the load magnitude, the RIKS method scales the applied loads proportionally by using λ.
- The solver estimate λ as part of the solution process with the displacements.
- The total load at any point during the analysis is given by:

$$P_{total} = P_0 + \lambda(P_{ref} - P_0)$$

Where P_0 is the initial load applied before the RIKS step, P_{ref} is the reference load and P_{tot} is the total load vector, and λ is the load proportionality factor.

- The RIKS method solves instantaneously for λ and the displacements, allowing it to track the load-displacement response even in regions where the load decreases.

Arc length is the geometric distance along the load-displacement curve as shown in Figure 5.2. This arc-length is a curve that measures the history of load-deflection curve regardless of whether the load or displacement is increasing or decreasing.

In order to understand these concepts, the steps to realise RIKS approach to solve the problem is as follows:

- Load Proportionality Factor (λ) see section 5.4: Determines the slope and adjusts your step to stay balanced and keep progressing.
- Arc Length (l): Tracks how far it is travelled along the path, ensuring that following the intended path and not going off or getting stuck.
- End of the Solution: Happens the trail is reached its end (termination criteria), whether it's a peak, a valley, or a specific waypoint.

5.4.3 Load Proportionally Factor (LPF)

The Load Proportionality Factor (LPF) is a main result in the RIKS method. It represents how much the reference load, defined in the previous section, is scaled during the analysis.

It also provides a direct measure of how the applied load progresses as the structure deforms.

When combined with displacement data, the LPF forms a load-displacement curve, which is crucial for understanding two critical aspects of buckling behaviour: the critical buckling load (the peak of the curve) and the post-buckling behaviour (how the structure responds after the peak, either stabilizing or collapsing).

The LPF diagram is in fact the representation of the load-displacement curve, designed to show how the structure's load capacity changes with increasing displacement.

The horizontal axis represents the displacement at a critical point on and indicating the magnitude of deformation of the structure. While the vertical axis represents the LPF (λ), which scales the reference load. By multiplying the LPF by the reference load total load can be calculated the at any stage of the analysis.

The diagram has several main structures:

- The peak point indicates the critical buckling load with the first point of buckling.

- Whereas the descending branch of the curve shows post-buckling behaviour, showing whether the structure stabilises (plateau) or collapses (with further decreasing).
- Before reaching the peak, the structure is stable and can resist additional loads; however, after the peak, the stiffness reduces and total instability occurs manifestly.

LPF values directly can be extracted from the output and use the load-displacement curve.

The maximum LPF indicates the critical buckling load.

5.5 Practical Step by step procedure for nonlinear buckling in ABAQUS

It must be recalled that the modelling procedure, as previously showed (see chapter 4), is the same but before running the linear buckling, except that an operation which consists of a command to its input file added. Through this command, the model's node file will be saved and will be used in the nonlinear buckling analysis when the imperfection value is introduced.

5.5.1 Input file template

The following example shows a post- buckling analysis of a structure with an imperfection defined and by using a linear superposition of the buckling eigenmodes and involves two analysis runs with the same model definition and conditions.

The initial analysis run performs an eigenvalue buckling analysis with Abaqus/Standard to establish the probable collapse modes and writes them to the results file. 5abaqus manual)

First procedure [90]

```
*HEADING
Initial analysis run to write the buckling modes to the results file
*NODE
Data lines to define initial "perfect" geometry
…
**
*STEP
*BUCKLE
Data lines to define the number of buckling eigenmodes
*CLOAD and/or *DLOAD and/or *DSLOAD and/or *TEMPERATURE
Data lines to specify the reference load, P_ref
*NODE FILE, GLOBAL=YES, LAST MODE=n
U
*END STEP
```

The second analysis run introduces the imperfection and performs a post-buckling analysis employing the modified RIKS method in Abaqus/Standard.

```
*HEADING
Second analysis run to define the imperfection and perform the post-buckling
analysis
*NODE
```

```
Data lines to define initial "perfect" geometry
…
*IMPERFECTION, FILE=results file, STEP=step
Data lines specifying the mode number and its associated scale factor
…
**
*STEP, NLGEOM
*STATIC, RIKS
Data line to define incrementation and stopping criteria
*CLOAD and/or *DLOAD and/or *DSLOAD and/or *TEMPERATURE
Data lines to specify reference loading, P_ref
*END STEP
```

- **An alternative second** analysis run introduces the imperfection and performs a post-buckling analysis with Abaqus/Explicit.

```
*HEADING
Second analysis run to define the imperfection and perform the postbuckling
analysis
*NODE
Data lines to define initial "perfect" geometry
…
*IMPERFECTION, FILE=results_file, STEP=step
Data lines specifying the mode number and its associated scale factor
…
**
```

1. Display the Edit Step dialog box following the Procedure type: General; Static, RIKS), or Editing a step.

2 Configure the settings such as limit criteria, the maximum number of increments, the arc increment length, and whether to account for geometric nonlinearity as described in the following procedures.

The Configuration settings should be selected as follows:

1. Step dialog box, display the Basic tabbed page.
2. Description field, enter a short of the file.
3. Select the Nlgeom option: Nlgeom off to perform LBA current step and Nlgeom on to account for geometric nonlinearity during the step.

More details can be found in Linear and nonlinear procedures (ABAQUS).

4. Specify when the step is completed is needed. Choose one or both of the following options: - Maximum load proportionality factor; λ_{end}. Or Maximum displacement.

Otherwise, the analysis continues for the number of increments that you specify on the.

- **Details of the RIKS procedure**

Before submitting the buckling analysis job, the node coordinates for the different mode shapes must be written as output. This output will be consequently introduced as imperfections for the RIKS analysis so as to achieve a smoother transition to the post buckling region and surpass the bifurcation problem.

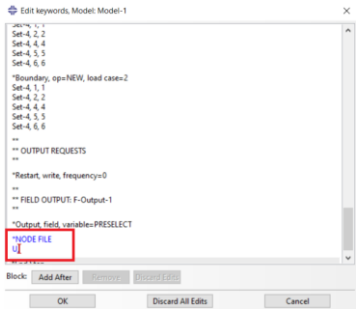


Figure 5.3 Introducing the node file command in the Buckle step

The changes needed for the new model to perform nonlinear buckling analysis are limited to adjustments in the Step and Load modules.

Additionally, modifications in the model's input file are required to include imperfections, which are essential for conducting nonlinear buckling analysis.

- **Defining Step Module:**

Go to the Step module and change the Step type to "Static, RIKS see figure 5.2.

Enable the nonlinear option and accept other settings as default.

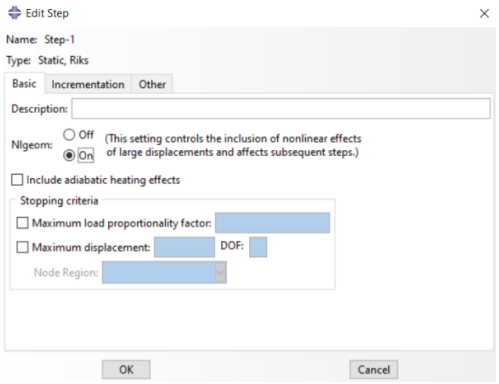


Figure 5.4 Selecting Static, RIKS Step

- **Performing Load Module:**

In the Load module, due to the change in analysis type, checks of loading conditions have been removed.

Next phase, is to introduce imperfections to the model

- **Addition of Imperfection and running the Analysis:**

To perform this task, open the model's input command file and enter the required command (see Figure below). The filename in the command signifies the Job name from the linear buckling

analysis, and the Step specifies which step of the analysis the command should be applied to. In the following three lines, you define the magnitude of the imperfections. If the Node File command wasn't used during the linear analysis, the run will result in an error.

N.B. In most cases, the magnitude of the imperfections is about one-tenth of the shell's thickness.

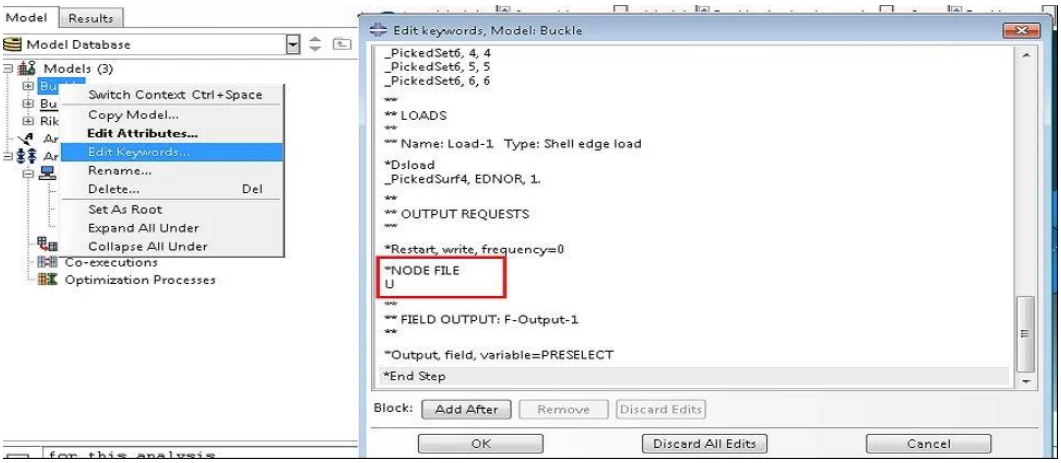


Figure 5.5 Addition of Imperfection commands in input file

Running: all set and you just have to run the analysis and see the results. The results depend on mesh convergence and most of all the imperfections introduced.

5.5.2 Demonstration

The element type used in this study is the shell with 8 nodes per element with 6 degrees of freedom for each node (three displacements in x, y, and z directions, and three rotations about x, y, and z-axes). While all elements, nodes, and loads are in x, y plane, in buckling analyses the out-of-plane displacements of all nodes other than the ones at the edges are not restrained.

Case of single circular web-opening

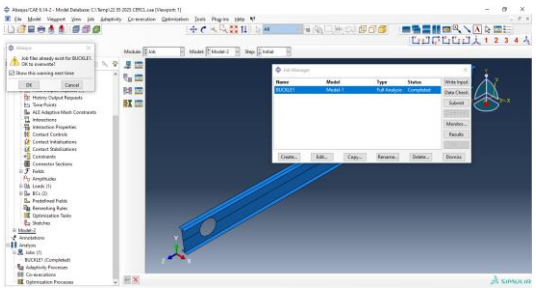


Figure 5.6 Executing the linear buckling analysis

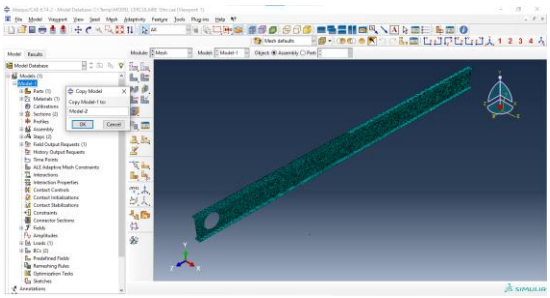


Figure 5.7 Copy the model

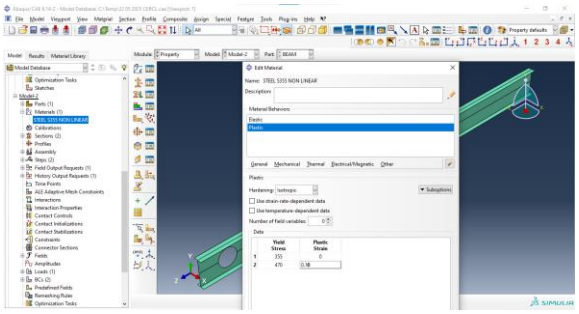


Figure 5.8 Material properties

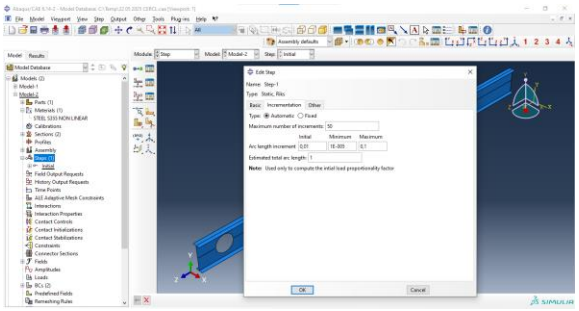


Figure 5.9 Performing RIKS analysis

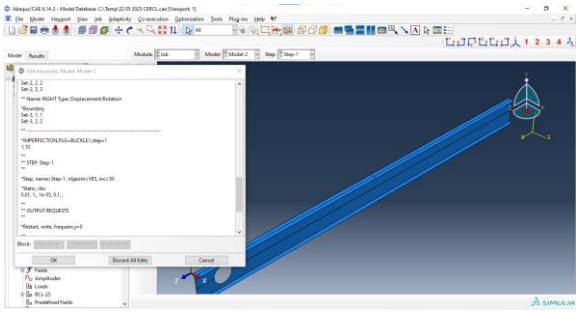


Figure 5.10 Introducing the imperfection as per EC3 (1/1000)

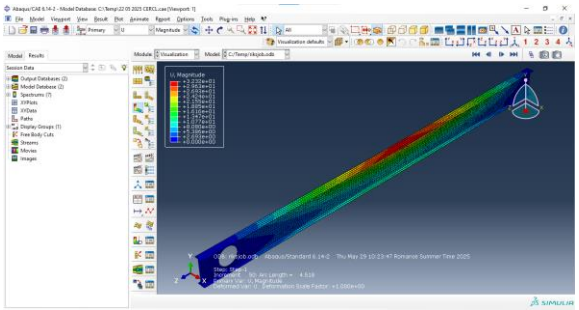


Figure 5.11 Deformed shape at ultimate increment

5.6 Studied cases

This research work deals with linear and nonlinear LTB strength of single and multi-web-opening steel structures. The shape of holes varies from circular, square to rectangular geometrical forms.

The first step of this work has been fully described and discussed in the previous chapter (i.e. Chapter 4). Concerning the linear lateral torsional buckling which was conducted successfully.

As mentioned above, time has come to perform more complicated analysis, with more advanced material, using ABAQUS software, that is the nonlinear post-buckling analysis. Detailed procedure of how to perform a full nonlinear post-buckling analysis taking into account geometric and material nonlinearity is described in previous section with the case of a single circular web-opening case. This step of my work is, in fact, an introduction to the nonlinear modelling of structures. An insight of the nonlinear buckling behaviour is an advanced topic needing a considerable amount of theoretical and numerical backgrounds. Lot of difficulties have risen when the nonlinear modelling begun. As an

The documents available in the Net including videos and guides explaining how to perform the nonlinear analysis are often incomplete and sometimes misleading by missing out very valuable information.

The parametric nonlinear analysis undertaken in this work considers several parameters: the shape and the size of the web-opening along with their number and locations for a simply supported unrestrained steel beam with the same cross section and material characteristics.

Single opening:

Case of circular single opening: Figure 5.12 and 5.13

For the first model build-up in ABAQUS, defaults parameters have been used to perform the nonlinear analyse. Although, the analysis was successfully completed in both steps, with no errors, unfortunately, results where far from expected real behaviour. Only the using circular web-opening gives acceptable results with 50 increments, the magnitude of imperfection as 10 mm, and 0.1 for ε_u. In this figure, a clear linear clear is visibly noticeable elastic behaviour up to about 18mm as a limit for elastic behaviour and subequal kind of post-buckling is noticeable with a decrease of the stiffness when the displacements are in the range (20 - 40 mm) and a form of plateau with slightly decreasing curve up to 100 mm. The value of the load at the bifurcation point about 90 kN which is approximately 1.25 time the value introduced value computed by the elastic buckling analyse indicating a post-buckling behaviour. Figure 5.12 and 5.13 show the results.

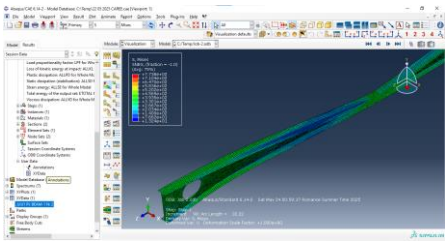


Figure 5.12 ultimate increment for single circular opening

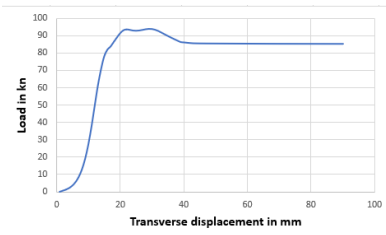


Figure 5.13 Load-deflection curve

In spite that I have strictly followed the procedure described in the case of single circular opening, the results for the remaining cases were quite different. In all cases, the load-displacement curves do not show any kind of a post-buckling behaviour with maximum transverse of 10 mm regardless the changes in imperfection, number of maximum increments and the input values of LFP with of courses of critical loads depending on the case in the position of bifurcation point. It seems that no post-buckling phenomenon is predicted, in contrast, it shows some kind of stability that beams experienced with a positive stiffness. This operation takes couple of weeks. More than 70 models have been build-up with different parameters., fruitlessly.

It seems, also, that the geometric nonlinearity is not operating. Although, in all running jobs, for different studied cases, the first step of nonlinear analysis give the same values of M_{cr} for linear torsional buckling which indicates that the subsequent analysis, that is nonlinear analysis will need beside the combinations of buckling modes the value of the imperfection (1/1000) of the span length.

The results are displayed in:

Case of square single opening: Figure 5.14 and 5.15

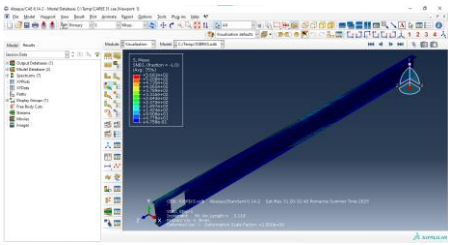


Figure 5.14 ultimate increment for single square opening

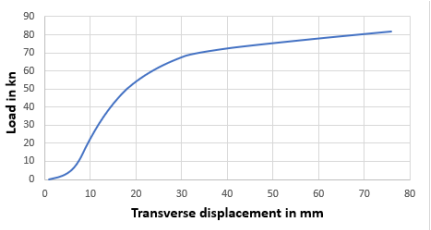


Figure 5.15 Load-deflection curve

Case of rectangular opening: Figure 5.16 and 5.17

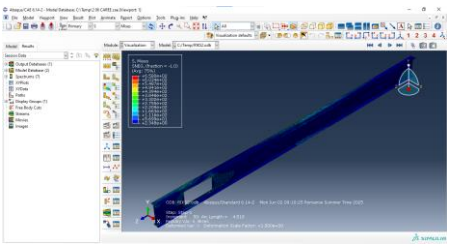


Figure 5.16 ultimate increment for single rectangular opening

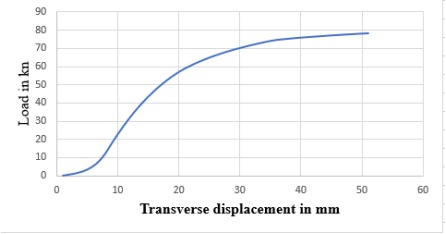


Figure 5.17 Load-deflection curve

Multi-opening:

Case of multi-circular opening: Figure 5.18 and 5.19

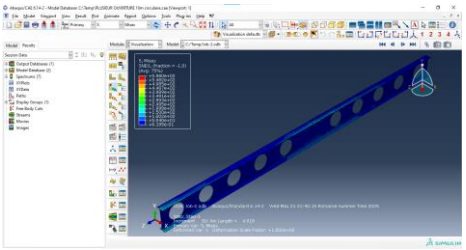


Figure 5.18 ultimate increment for multi-circular opening

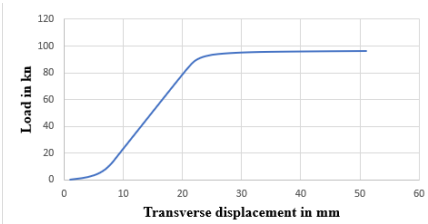


Figure 5.19 Load-deflection curve

Case of multi-rectangular opening: Figure 5.20 and 5.21

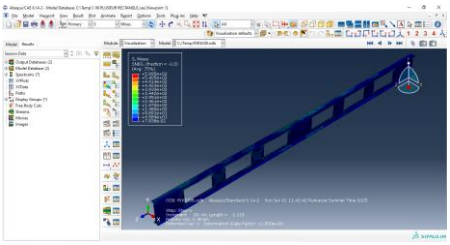


Figure 5.20 ultimate increment for multi- rectangular opening

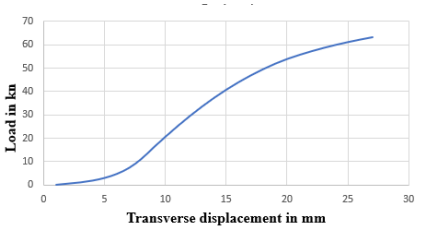


Figure 5.21 Load-deflection curve

Generally speaking, from interpreting the whole results, it can be said that nonlinear analysis gives higher values of the critical loads than it was in the linear buckling analysis, which means that the LBA gives conservative values.

Thinking that the introduced imperfection value was smaller than it should be changing the imperfection with higher values to access their effect on the post-buckling behaviour has not solve the problem. Changing the number of increments from 50, 75 up to 99 has not given better results. This operation takes couple of weeks. More than 70 models have been build-up with different parameters., fruitlessly.

SUMMARY, CONCLUSIONS AND RECOMMENDATIONS FOR FUTURE WORK

CONCLUSIONS AND RECOMMENDATIONS FOR FUTURE WORKS

A- Conclusions

From this work, some conclusions can be drawn in two parts:

Part 1 Dissertation

1. I have learned much about the particular case of castellated beams: their description, mode of failure and specially their buckling behaviour.
2. The updated literature review gives me the opportunity to make my first steps in a research work by reading and summarising the papers.
3. Also, my background of finite element method has been improved regarding its concepts and particularly its application in solving buckling problems.
4. An insight in advanced topics such as the nonlinear buckling was a precious background.
5. Modelling in tri-dimensional using the general purpose ABAQUS was very helpful to understand the basics and more advanced techniques of modelling. I have learned the impact of support conditions, the choosing of type element, the number of incrementations etc.

Part 2 From the parametric analysis performed on a simply supported unrestrained beam in this work:

1. The geometric shape of the opening was a determinant factor in both linear and nonlinear LTB resistance of WOB. The circular form of hole has been shown in this work to be the best configuration compared to the square which is close and the worst case the rectangular one.
2. The impact of sensitivity to imperfection was show to be a key parameter in nonlinear analysis along with the eigen values.
3. For single circular, an acceptable curve was obtained showing clearly an elastic then an inelastic behaviour with a post-buckling behaviour.
4. For the remaining case including those with single opening gave curves with elastic branch and stop when the bifurcation point is attained. This visibly needs a further investigation to clarify the problem.

B- Recommendations for future works

1. A comparative analysis using other software, i.e. ANSYS to check the results obtained in this research work to see how the accuracy of the results.
2. Carry out other investigation of 3D linear a nonlinear LTB for restrained structures under static loadings.

3. It seems that an exploring the dynamic response of WEB associated with the LTB considerations.
4. Study the LTB of castellated beam used in composite structures.

References

[1] teaching resources for structural steel design (volume 1,2 & 3 - chapter 28:"steel beams with web openings" prepared jointly by: experimental investigation for failure analysis of steel beams with web openings indian institut of technology, madras anna university, chennai, structural engineering research centre, madras, institute for steel development and growth

[2] Marwa Boudjadja 3d numerical investigation of the linear and non-linear performance of steel structures having web openings under different loading conditions Master Academic Dissertation 2020

[3] J.G. Verweij; Master's thesis: "CELLULAR BEAM-COLUMNS IN PORTAL FRAME STRUCTURES", Delft University of Technology, Civil Engineering Section, Steel and Timber Structures, November 2010.

[4] Chapter I: Introduction and Literature Review Link https://vtechworks.lib.vt.edu/bitstream/handle/10919/31117/ChapterI.pdf

[**5**] castellated beams – an overview link https://www.steel-insdag.org/uploads/filemanager/16778367680p.pdf

[6] what is a castellated beam? advantages, sizes, design, & ... link ... https://www.c-beams.com/what-is-castellated-beam/

[**7**] S. S. Fares, J. Coulson, and D. W. Dinehart, "Design Guide 31: Castellated and Cellular Beam Design", American Institute of Steel Construction, Chicago, IL, USA, 2016.

[8] ArcelorMittal Commercial Sections S.A., "ACB® and Angelina™ Beams - A New Generation of Castellated Beams", ArcelorMittal, 2015.

[9] Ahmad Razin Zainal Abidin; "Modelling of Local Elastic Buckling for Steel Beams with Web Openings", MSc thesis, Imperial College London, Department of Civil and Environmental Engineering, January 2013.

[10] D. Sonck and J. Belis, "Lateral-Torsional Buckling Resistance of Cellular Beams", Journal of Constructional Steel Research, Vol. 105, pp. 119–128, 2015, doi: 10.1016/j.jcsr.2014.11.003.

[11] F. Erdal and M. P. Saka, "Ultimate load carrying capacity of optimally designed steel cellular beams," *Journal of Constructional Steel Research*, vol. 80, pp. 355–368, Jan. 2013, doi: 10.1016/j.jcsr.2012.10.007.

[12] Eurocode 3 Version ENV, "Calcul des Structures en Acier" and National Application Document, 2002.

[13] D. Kerdal and D. Nethercot, "Failure Modes for Castellated Beams", Journal of Constructional Steel Research, Vol. 4, No. 4, pp. 295–315, 1984.

[14] R. Manfred and A. Hirt, "Construction Métallique : Notions Fondamentales et Méthodes de Dimensionnement", Traité de Génie Civil de l'École Polytechnique Fédérale de Lausanne – Vol. 10, 1994.

[15] S. Demirdjian, "Stability of Castellated Beam Webs", Master's thesis, McGill University, Montréal, Canada, p. 140, March 1999.

[16] K. Tsavdaridis and c. D'mello, "web buckling study of the behaviour and strength of perforated steel beams with different novel web opening shapes", journal of constructional steel research, vol. 67, no. 10, pp. 1605–1620, 2011.

[17] S. Durif, "Comportement Mécanique des Poutres Cellulaires à Ouvertures Sinusoïdales - Développement d'un Modèle Analytique Adapté", PhD Thesis, Université Blaise Pascal, Clermont-Ferrand, p. 279, 2012.

[18] D. Kerdal, "Lateral Torsional Buckling Strength of Castellated Beams", PhD Thesis, University of Sheffield, p. 280, November 1982.

[19] H. Bouzid, "Étude Paramétrique du Comportement Élastique « En Flexion Simple » des Poutres Métalliques Ajourées", The 13th Arab Structural Engineering Conference, University of Blida 1, Algeria, pp. 1–7, December 13-15, 2015.

[20] M. Knobloch and M. Fontana, "Strain-Based Approach to Local Buckling of Steel Sections Subjected to Fire", Journal of Constructional Steel Research, Vol. 62, No. 1-2, pp. 44-67, 2006.

[21] Hassan -Rasul-2013 Distortional Lateral Torsional Buckling Analysis for Beams of Wide Flange Cross-Sections Department of Civil Engineering Faculty of Engineering University of Ottawa

[22] M.A. Bradford, Buckling of elastically restrained beams with web distortions, Thin-Walled Struct. 6 (1988) 287–304, https :// doi.org / 10 .1016 / 0263 - 8231 (88) 90005-5.
[23] J.N. Goodier, M.V. Barton, The effects of web deformation on the torsion of I beams, J. Appl. Mech. (1944) A-35–A-40.
[24] G.J. Local Hancock, Distortional, and lateral buckling of I-beams, J. Struct. Div. 104 (1978) 1787–1798.
[25] T.M. Roberts, P.S. Jhita, Lateral, local and distortional buckling of I-beams, Thin-Walled Struct. 1 (1983) 289–308, https://doi.org/10.1016/0263-8231(83)90011-3.
[26] H.R. Naderian, H.R. Ronagh, M. Azhari, Elastic distortional buckling of doubly sym-metric steel I-section beams with slender webs, Thin-Walled Struct. 84 (2014).289–301, https://doi.org/10.1016/j.tws.2014.05.010
[27] S. Tohidi, Y. Sharifi, Neural networks for inelastic distortional buckling capacity as-sessment of steel I-beams, Thin-Walled Struct. 94 (2015) 359–371, https://doi. org/10.1016/j.tws.2015.04.023.
[28] A. Samanta, A. Kumar, Distortional buckling in braced-cantilever I-beams, Thin-Walled Struct. 46 (2008) 637–645, https://doi.org/10.1016/j.tws.2007.12.004.
[29] K.J.R. Rasmussen, X. Zhang, H. Zhang, Beam-element-based analysis of locally and/or distortionally buckled members: theory, Thin-Walled Struct. 98 (2016) 285–292, https://doi.org/10.1016/j.tws.2015.06.020.
[30] Z. Vrcelj, M.A. Bradford, Elastic distortional buckling of continuously restrained I-section beam-columns, J. Constr. Steel Res. 62 (2006) 223–230, https://doi.org/10. 1016/j.jcsr.2005.07.014.
[31] A. Samanta, A. Kumar, Distortional buckling in monosymmetric I-beams, Thin-Walled Struct. 44 (2006) 51–56, https://doi.org/10.1016/j.tws.2005.09.007.
[32] T. Zirakian, Elastic distortional buckling of doubly symmetric I-shapedflexural members with slender webs, Thin-Walled Struct. 46 (2008) 466–475, https://doi.
[33] I. Kalkan, A. Buyukkaragoz, A numerical and analytical study on distortional buck-ling of doubly-symmetric steel I-beams, J. Constr. Steel Res. 70 (2012) 289–297, https://doi.org/10.1016/j.jcsr.2011.06.006.
[34] Y.-L. Pi, N.S. Trahair, Distortion and warping at beam supports, J. Struct. Eng. 126 (2000) 1279–1287, https://doi.org/10.1061/(ASCE)0733-9445(2000)126:11(1279).
[35] M.A. Bradford, Distortional buckling of monosymmetric I-beams, J. Constr. Steel Res. 5(1985)123–136, https://doi.org/10.1016/0143-974X(85)90010-0.
[36] M.A. Bradford, Inelastic distortional buckling of I beams, Comput. Struct. 24 (1986) 923–933, https://doi.org/10.12989/scs.2003.3.1.001.
[37] M.A. Bradford, Buckling strength of deformable monosymmetric I-beams, Eng. Struct. 10 (1988) 167–173, https://doi.org/10.1016/0141-0296(88)90003-X.
[38] C.M. Wang, C.K. Chin, S. Kitipornchai, Parametric study on distortional buckling of monosymmetric beam-columns, J. Constr. Steel Res. 18 (1991) 89–110, https:// doi.org/10.1016/0143-974X (91)90067-B.
[39] Y.-L. Pi, N.S. Trahair, Lateral-distortional bucklingof hollowflangebeams, J. Struct. Eng. 123 (1997) 695–702, https://doi.org/10.1061/(ASCE)0733-9445(1997)123:6(695).
[40] M.A. Bradford, Lateral-distortional buckling of steel I-section members, J. Constr. Steel Res. 23 (1992) 97–116, https://doi.org/10.1016/0143-974X(92)90038-G.
[41] Sonck, D., & Belis, J. (2015). Lateral-torsional buckling resistance of cellular beams. Journal of Constructional Steel Research, 105, 119-128.
[42] Nimmi, K. P., & Krishnachandran, V. N. (2016). *Buckling analysis of cellular steel beams with and without stiffeners*. International Journal for Research in Applied Science & Engineering Technology, August.
[43] Elaiwi, S. S., Kim, B., & Li, L. Y. (2019). Linear and nonlinear buckling analysis of castellated beams. International Journal of Structural and Civil Engineering Research, 8(2).
[44] Ferreira, F. P. V., Rossi, A., & Martins, C. H. (2019). Lateral-torsional buckling of cellular beams according to the possible updating of EC3. Journal of Constructional Steel Research. https://doi.org/10.1016/j.jcsr.2018.10.011

[45] Boissonnade, N., Nseir, J., & Somja, H. (2024). Experimental and numerical investigations towards the lateral torsional buckling of cellular steel beams. Thin-Walled Structures, 195, 111388. https://doi.org/10.1016/j.tws.2023.111388
[46] Zewudie, B. B., Zerfu, K., & Agon, E. C. (2024). Numerical investigation of elastic-plastic buckling performance of circular arched cellular steel beam using nonlinear finite element analysis method. Heliyon, January 2024.
[47] Nassim, K., Benyamina, A. B. B., & Lyacine, B. (2024). Effect of reliability and lateral-torsional buckling of steel beams in the linear and non-linear domain. Brazilian Journal of Technology, 7(3), 01–27.
[48] Piassi, A. D., Dias, J. V., Calenzani, A. F. G., & Menandro, F. C. C. (2018). Lateral distortional buckling of cellular composite-beams. Revista IBRACON de Estruturas e Materiais, 11(2), 331–356. http://dx.doi.org/10.1590/S1983-41952018000200007
[49] Rajana, K., Tsavdaridis, K. D., & Koltsakis, E. (2020). Elastic and inelastic buckling of steel cellular beams under strong-axis bending. Thin–Walled Structures, 156, 106955.
[50] Rossi, A., Ferreira, F. P. V., Martins, C. H., & Mesacasa Júnior, E. C. (2020). Assessment of lateral distortional buckling resistance in welded I-beams. Journal of Constructional Steel Research, 166, 105924.
[51] Hosseinpour, M., & Sharifi, Y. (2021). Finite element modelling of castellated steel beams under lateral-distortional buckling mode. Structures, 29, 1507–1521.
[52] Gamal, H., El-Boghdadi, M., Hassanein, M. F., & EL Hadidy, A. M. (2019). *The lateral distortional buckling of I-plate girders*. Journal of Engineering Research, 3(4).
[53] Saternus, P. (2022). *Cellular beams with closely spaced web openings – A review of analytical calculation models for web-post buckling*. Advances in Science and Technology Research Journal, 16(1).
[54] Silva de Carvalho, A., Moura de Oliveira, V., Rossi, A., & Martins, C. H. (2023). Elastic lateral-torsional buckling behaviour of steel I-beams with sinusoidal web openings.

[55] Kurlapkar, R. R., Jadhav, V., & Hasabe, A. (2025). Lateral-torsional buckling behaviour of castellated steel beams with sinusoidal web openings: A parametric study. Asian Journal of Civil Engineering, 26, 1583–1594. https://link.springer.com/article/10.1007/s42107-025-01268-0
[56] M. Maali , N. Çınar Experimental and Numerical Tests on Beams with Web Openings Under Cyclic Loading. AJCE 29 August 2024.
[57] Kamal, A.I.A., Zakwan, F.A.A. & Ismail, R Flexural behavior of cellular stainless-steel beams: experimental and statistical analysis. AJCE 22 April 2025.
[58] Taher Al-Dafafea. Analyses expérimentale et numérique du comportement de poutres à ouvertures d'âmes raidies. Génie civil. Université Clermont Auvergne [2017-2020], 2018. Français. ffNNT : 2018CLFAC024ff. fftel-02088539

[59] A. Marneffe, "Calcul direct de la poutre Vierendeel par la méthode des systèmes équivalents l'ellipse," IABSE Publications, vol. 31, no. 5, pp. 233-260, 1937.
[60] E. Robert and L. Musette, "Note sur le calcul des poutres Vierendeel," IABSE Publications, vol. 15, pp. 187–198, 1955.
[61] R. Lawson and S. Hicks, "Design of composite beams with large web openings," SCI Publication 355, 2011.
[62] R. Redwood and S. Ho Cho, "Design of steel and composite beams with web openings," Journal of Constructional Steel Research, vol. 25, pp. 23–41, 1993.
[63] K. Tsavdaridis and C. D'Mello, "Vierendeel bending study of perforated steel beams with various novel web opening shapes through nonlinear finite-element analyses," Journal of Structural Engineering, vol. 138, no. 10, pp. 1214–1230, 2012.
[64] K. Chung and R. M. Lawson, "Simplified design of composite beams with large web openings to Eurocode 4," Journal of Constructional Steel Research, vol. 57, no. 2, pp. 135–163, 2001.
[65] R. Shrivastava and S. Redwood, "Web instability near reinforced rectangular holes," IABSE proceedings, vol. 1, no. 6, pp. 1-17, 1977.

[66] K. Chung, T. Liu, and A. Ko, "Investigation on Vierendeel mechanism in steel beams with circular web openings," Journal of Constructional Steel Research, vol. 57, no. 5, pp. 467–490, 2001.
[67] T. Liu and K. F. Chung, "Steel beams with large web openings of various shapes and sizes: Finite element investigation," Journal of Constructional Steel Research, vol. 59, no. 9, pp. 1159–1176, 2003.
[68] D. Darwin, "Design of composite beams with web openings," Progress in Structural Engineering and Materials, vol. 2, no.2, pp. 157–163, April 2000.
[69] W. Lucas and D. Darwin, "Steel and composite beams with web openings," The American Iron and Steel Institute, The University of Kansas, p. 188, June 1990.
[70] R. Hoffman, D. Dinehart, S. Gross, and J. Yost, "Analysis of stress distribution and failure behavior of cellular beams," International ANSYS Conference, 2-4 May 2006.
[71] L. Budi, Sukamta, and W. Partono, "Optimization analysis of size and distance of hexagonal hole in castellated steel beams," Procedia Engineering, vol. 171, pp. 1092–1099, 2017.

[72] R. Frans, H. Parung, D. Sandy, and S. Tonapa, "Numerical modelling of hexagonal castellated beam under monotonic loading," Procedia Engineering, vol. 171, pp. 781–788, 2017.

[73] P. Martin, M. Couchaux, O. Vassart, and A. Bureau, "An analytical method for the resistance of cellular beams with sinusoidal openings," Engineering Structures, vol. 143, pp. 113–126, 2017.

[74] L. Zhang and P. Wang, "Simplified analysis method for catenary action of restrained cellular steel beams at elevated temperature considering strain reversal," Fire Safety Journal, vol. 95, pp. 145–159, November 2018.

[75] BSI (British Standards Institution), "Eurocode 3: Design of steel structures - Part 1.2: General rules - Structural fire design," July 2003.
[76] EN 1993-1-3, Eurocode 3 - Design of steel structures - Part 1-3: General rules - Supplementary rules for cold-formed members and sheeting, 2006.
[77] H. Showkati, T. Ghazijahani, A. Noori, and T. Zirakian, "Experiments on elastically braced castellated beams," Journal of Constructional Steel Research, vol. 77, pp. 163-172, 2012.
[78] Anupriya and K. Jagadeesan, "Shear strength of castellated beam with and without stiffeners using FEA (ANSYS 14)," International Journal of Engineering and Technology, vol. 6, no. 4, pp. 1970-1981, 2014.
[79] P. Panedpojaman and T. Rongram, "Design equations for Vierendeel bending of steel beams with circular web openings," Proceedings of the World Congress on Engineering, vol. II, no. C, pp. 978-988, 2014.
[80] R. M. Lawson, J. Lim, S. J. Hicks, and W. I. Simms, "Design of composite asymmetric cellular beams and beams with large web openings," Journal of Constructional Steel Research, vol. 62, no. 6, pp. 614–629, 2006.
[81] O. Vassart, "Analytical Model for Cellular Beams Made of Hot Rolled Sections in Case of Fire," PhD Thesis, Université Blaise Pascal, Clermont-Ferrand, p. 189, 2009.
[82] R. Maquoi and M. Skaloud, "Stability of Plates and Plated Structures: General Report," *Journal of Constructional Steel Research*, vol. 55, no. 1, pp. 45–68, September 2000.
[83] EN 1993-1-5, *Eurocode 3 - Design of Steel Structures - Part 1-5: Plated Structural Elements*, 2004
[84] B. Johansson, R. Maquoi, G. Sedlacek, C. Müller, and D. Beg, "Commentary and Worked Examples to EN 1993-1-5 (Plated Structural Elements)," vol. 1, October 2007.
[85] A. Nadjai, O. Vassart, F. Ali, D. Talamona, A. Allam, and M. Hawes, "Performance of Cellular Composite Floor Beams at Elevated Temperatures," *Fire Safety Journal*, vol. 42, no. 6–7, pp. 489–497, 2007.
[86] M. Azhari and M. Bradford, "Local Buckling of I-Section Beams with Longitudinal Web Stiffeners," *Thin-Walled Structures*, vol. 15, no. 1, pp. 1–13, 1993.

[87] J. Lu and H. Lieurade, “Stress Concentration,” *Techniques de l’Ingénieur, Mechanical Engineering Series*, vol. 33, pp. 1–24, 1998.
[88] Khennane. A, 2013 Introduction to finite element analysis using MATLAB{\textregistered} and abaqus. (C. Press, Éd).
[89] Finite Element Analysis and DESIGN OF META STRUCTURES EHAB ELLOBODY, RAN FENG, BEN YOUNG ISBN: 978-0-12-416561-8 2014
[90] Abaqus Analysis User’s Manual Volume II 2012